Journal of Modern Technology & Engineering
Vol.3, No.1, 2018, pp.15-52

FREE AND FORCED VIBRATIONS OF LIQUID STORAGE TANKS WITH BAFFLES

Elena Strelnikova[1,2*], Vasyl Gnitko[1], Denys Krutchenko[1], Yury Naumemko[1]

[1] A.N. Podgorny Institute for Mechanical Engineering Problems, Kharkiv, Ukraine
[2] V.N. Karazin Kharkiv National University, Kharkiv, Ukraine

Abstract. In this paper we consider vibrations of shells of revolution partially filled with a liquid. The liquid is supposed to be an ideal and incompressible one and its flow introduced by the vibrations of the shell is irrotational. The problem of the fluid-structure interaction is solved using single-domain and multi-domain reduced boundary element methods. The rigid and elastic baffled tanks with different annular orifices are considered. The dependencies of frequencies via orifice radius at different values of the filling level are obtained numerically for vibrations of the fluid-filled tanks with and without baffles.

Keywords: *fluid-structure interaction, baffles, liquid sloshing, free vibrations, boundary element method, singular integral equations.*

Corresponding Author: *Prof. Elena Strelnikova, Department of General Research in Power Engineering of A.N. Podgorny Institute for Mechanical Engineering Problems, 2/10 Pozharsky St., Kharkiv, 61046, Ukraine, e-mail: elena15@gmx.com*

Manuscript received: *10 August 2017*

1. Introduction

Practicing engineers face many issues and challenges on design and seismic simulation of liquid storage tanks. The liquid storage tanks are important components of lifeline and industrial facilities. Ground-supported cylindrical tanks are used to store a variety of liquids – water for drinking and firefighting, crude oil, wine, liquefied natural gas, etc. Failure of tanks, following destructive earthquakes, may lead to environmental hazard, loss of valuable contents, and disruption of fire-fighting effort. Inadequately designed or detailed tanks have suffered extensive damage in past earthquakes that has resulted in disastrous effects (see Jung *et al*., 2006; Malhotra, 1997; Ru-De, 1993; Sanchez-Sanchez *et al.*, 2004).

Liquid sloshing near free surfaces can damage roofs and upper shells of storage tanks. High stresses in the vicinity of poorly detailed base anchors can rupture the tank wall. Base shears can overcome friction causing the tank to slide.

Early simulations of the liquid sloshing problem relied upon constructing mechanical analogies that comprise pendulums or spring – mass elements whose parameters are designed to simulate the resultant dynamic pressure loads imparted on a tank during sloshing are presented in (Degtyarev *et al*., 2015; Degtyarev *et al*., 2016). Housner (Degtyarev *et al*., 2015) obtained classical solutions for impulsive and convective parameters of ground supported rectangular and circular tanks (under horizontal accelerations). The work was further extended to analyze elevated water tanks (Degtyarev *et al*., 2016). The tanks walls were considered rigid. It should be noted that engineering procedures for seismic analysis and design of storage tanks are often

based on the Housner multicomponent spring-mass analogy (Degtyarev *et al.*, 2015). The analogy allows the complex dynamic behaviour of the tank and its contents to be considered in a simplified form. The principal modes of response include a short period impulsive mode, with a period of around 0.5 seconds or less, and a number of longer period convective (sloshing) modes with periods up to several seconds. For most tanks, it is the impulsive mode that dominates the loading on the tank wall. The frequency of the first convective mode is usually much less than the impulsive one, and the higher order convective modes can be ignored. Later Veletsos and Yang (Veletsos & Yang, 1976) considered the effect of flexibility of cylindrical tanks.

Comprehensive reviews of the phenomenon of sloshing, including analytical predictions and experimental observations were done in the work of Abramson (Abramson, 1966) and Ibrahim (Ibrahim, 2005). Ibrahim also suggested in (Ibrahim, 2005) that exact solutions for the linear liquid sloshing are limited to regular tank geometries with straight walls, such as rectangular and upright-cylindrical containers. Note that fluid-free-surface natural frequencies and mode shapes for two- and three-dimensional rectangular tanks have been obtained by Abramson (Abramson, 1966) and Ibrahim (Ibrahim, 2005) using the method of separation of variables. Owing to difficulties associated with this classical method for analysis of linear slosh in most practical tank geometries (e.g., horizontal cylinders, spherical tanks), several other methods have been developed for linear slosh analysis.

Since analytic solutions do not exist for tanks and reservoirs with complicated geometrical shapes, in addition to the analytical methods, numerical methods have been employed for solutions of linear boundary value problems of liquid sloshing. The dynamic analysis of shell structures is often performed by use of finite element programs (Jung *et al.*, 2006).

Ru-De (Ru-De, 1993) presented a finite element analysis of linear liquid slosh in an upright cylindrical tank under a lateral excitation. Arafa in (Arafa, 2006) developed a finite element formulation to investigate the sloshing of liquids in partially filled rigid rectangular tanks undergoing base excitation. Hydro-elastic oscillations of rectangular plates, resting on Pasternak foundation and interacting with an ideal incompressible liquid with a free surface, are studied in (Kutlu *et al.*, 2012).

But such 3-D nonlinear finite element analysis, including the contained fluid as well as the foundation soil, and elasticity of the shell walls is complex and extremely time consuming. Several simplified theoretical investigations were also conducted, and other numerical methods were elaborated. Some of these studies have been used as a basis for current design standards.

Faltinsen and Timokha (Faltinsen & Timokha, 2012) developed a linear multimodal method to study the two-dimensional liquid slosh in a horizontal cylindrical tank. Based on the linear multimodal approach, the free-surface elevation and velocity potential were expressed by series of the natural sloshing modes. This reduced the associated linear boundary value problem to a set of ordinary differential equations. McIver (McIver, 1989) also solved the potential flow equation for the free liquid sloshing in two-dimensional cylindrical and spherical containers using the conformal mapping technique and reported the natural frequencies in terms of liquid filling level.

Ergin and Ugurlu (Ergin & Ugurlu, 2004), investigated the effects of different boundary conditions on the response behaviour of thin circular cylindrical shell structures fully in contact with flowing fluid using finite and boundary element methods.

The adequate definition of the fluid free-surface needs to be tracked using alternate methods such as the volume-of-fluid method This method was developed by Kim and Lee (Kim & Lee, 2003) and Kim et al. (Kim *et al*., 2003) on the basis of fractional volumes of liquid in a cell, which can be used to identify the position of the free-surface.

The viscous effects on sloshing frequencies were studied in (Bauer & Chiba, 2007)

To damp the liquid motion and prevent instability a lot of slosh-suppression devices have been proposed. Such devices are used to reduce structural loads induced by the sloshing liquid, to control liquid position within a tank, or to serve as deflectors. These devices include rigid or elastic ring baffles of various sizes and orientation, rectangular plates submerged into a fluid-filled tank, different plates partly covering the free surface. The selection and design of suppression systems require quantitative knowledge of the slosh characteristics.

In practice, the effect of baffles usually can be seen after the baffle has been installed. But often this experimental work is too expensive. So developing computational methods for qualified numerical simulation is a very topical issue. One of the pioneering papers in the area was written by Miles (Miles, 1958).

The linear sloshing in a circular cylindrical tank with rigid baffles has been studied by many authors in the context of spacecraft applications. Experimental and numerical results were reported in Watson (Watson & Evans, 1991).

Hasheminejad and Mohammadi (Hasheminejad & Mohammadi, 2011) employed the conformal mapping technique to study the effect of surface-touching horizontal side baffles, bottom mounted vertical baffle and surface piercing vertical baffle in cylindrical containers under lateral excitations. The study showed that a long pair of surface-touching horizontal side baffles have considerable effect on the natural sloshing frequencies while the bottom mounted vertical baffle was not recommended as an effective anti-sloshing device. A surface-piercing vertical baffle, however, was found to be efficient for controlling the liquid sloshing under high fill levels. The same conclusion was also drawn by Hasheminejad and Aghabeigi (Hasheminejad & Aghabeigi, 2009, 2011, 2012) where elliptical tanks with the same baffle configurations were considered.

Cho et al. (Cho & Lee, 2004; Cho *et al*., 2005) and Arafa (Arafa, 2006) developed a finite element formulation for linear liquid slosh in two-dimensional baffled rectangular tanks. Also finite element method was applied in (Arafa, 2006; Cho & Lee, 2004; Cho *et al.*, 2005) to examine numerically the damping effects of disc-type elastic baffle on the dynamic characteristics of cylindrical fuel-storage tank boosting with uniform vertical acceleration.

Askari et al. (Askari *et al.*, 2011) developed an analytical method to investigate the effects of a rigid internal body on bulging and sloshing frequencies and modes of a cylindrical container partially filled with a fluid using the Rayleigh quotient, Ritz expansion, and Galerkin method. Askari and Daneshmand (Askari & Daneshmand, 2009) proposed finite element method using Galerkin method to analysis coupled vibrations of a partially fluid-filled cylindrical container with a cylindrical internal body.

The effects of baffles on the natural sloshing frequencies were also investigated by Gedikli and Erguven (Gedikli & Erguven, 2003) using a variational boundary element method (BEM). Gedikli and Erguven (Gedikli & Erguven, 1999) also reported

seismic responses for an upright cylindrical tank with a ring baffle using BEM and superposition of modes. The major contribution of these works was the significant reduction of computational cost compared to other numerical methods such as the finite element method. Gedikli and Erguven in (Gedikli & Erguven, 1999, 2003) used BEM to investigate the sloshing problem using Hamilton method and evaluated the influence of baffle size and location on natural frequencies of upright rigid cylindrical tank.

So then boundary integral equations have been widely used for the solution of a variety of problems in engineering. This approach has certain advantages. In the basic equations the functions and their derivatives will be defined on the domain boundaries only. That allows reducing the problem dimension. This method gives new qualitative possibilities in modeling dynamic coupled problems.

Though BEM formulations have provided robust solutions to engineering problems, the resulting discretized systems are typically dense and non-symmetric, thus entailing increased computational cost especially when compared to domain discretization methods. It was the reason that multi-domain methods, or domain decomposition methods based exclusively on boundary elements have also appeared for both interior and exterior boundary value problems (Brebbia, 1984; Crotty, 1982; Rigby and Aliabadi, 1995). The main idea of multi-domain is in dividing the original domain into smaller ones (sub-domains or macro-elements). In each domain the BEM formalism is employed. Fictitious (interface) boundaries are involved to delimit the domains when necessary and will be described in terms of pressure and velocity similar to solid boundaries. Continuity equations are written on these fictitious boundaries. Then the BEM algebraic equations are established for each sub-domain; and the global system of equations is formed by assembling results of all sub-domains in terms of the equilibrium and consistence conditions over common interface nodes. The Blocked Equation Solvers (Crotty, 1982; Rigby & Aliabadi, 1995) are proposed to obtain the solutions of these sparse systems of algebraic equations.

The multi-domain BEM is especially effective at numerical simulation of tanks with baffles.

When liquids slosh in closed containers, one can observe the multiple configurations (modes) in which the surface may evolve. Commonly, the different modes can be defined by their wave number α (number of waves in the circumferential direction) and by their mode number *n*.

Although baffles are commonly used as the effective means of suppressing the sloshing magnitudes, the only few studies have assessed the role of baffle design factors. The size and location effects of a baffle orifice on the sloshing has been reported in only two studies devoted rectangular Popov et al (Popov, 1993) and generic Guorong et al. (Guorong & Rakheja, 2009) cross-section tanks.

It should be noted that anti-slosh properties of baffle designs have been investigated through laboratory experiments by using small size tanks of different geometry Lloyd et al. (Lloyd *et al*., 2002).

The overview of the research on the topic (Bermudez & Rodrigues, 1999; Guorong & Rakheja, 2009; Jung *et al*., 2006; Lloyd *et al.*, 2002) demonstrates that the dynamic response of liquid-containing structures can be significantly influenced by vibrations of their elastic walls in interaction with the sloshing liquid.

In (Degtyarev *et al.*, 2015, 2016; Gnitko *et al.*, 2016, 2017; Strelnikova *et al*., 2016; Ventsel *et al*., 2010) the authors developed an approach based on using the coupled finite and boundary element method to the problem of natural vibrations of the

fluid-filled elastic shells of revolution, as well as to the problem of natural liquid vibrations in the rigid vessels. But in (Degtyarev *et al.*, 2016; Gnitko *et al.*, 2016; Strelnikova *et al.*, 2016) the only rigid vessels were under consideration. In (Ventsel *et al.*, 2010) the fluid-structure interaction was considered without including the sloshing effects, and in (Degtyarev *et al.*, 2015; Gnitko *et al.*, 2017) the effects of sloshing and elasticity of walls were considered separately.

This paper is summarizing the authors' efforts in the area. We consider here free and forced liquid vibrations in cylindrical, conical and spherical tanks with and without baffles, carry out the numerical simulation of elasticity effects, and mutual influence of sloshing and elasticity of tank walls on the frequencies.

2. Problem statement

Consider a coupled problem of dynamic behavior of an elastic shell of revolution partially filled with a liquid under a short-time impulsive load. Also free and forced vibrations of such shells are under consideration.

Suppose that the fluid-filled elastic shell of revolution of an arbitrary meridian has internal baffles installed to damp the liquid sloshing. The shell is of uniform thickness h, and height L, made of homogeneous, isotropic material with elasticity modulus E, Poisson's ratio ν and mass density ρ_s. The shell structure and its sketch are shown in Fig. 1.

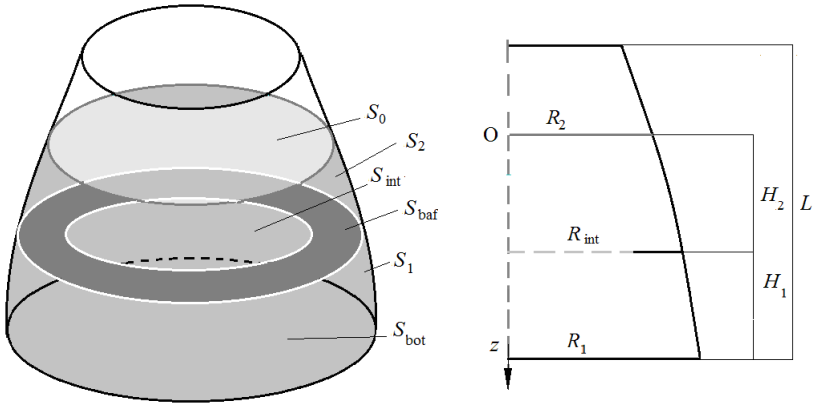

Figure 1. Shell structure with an internal baffle and its sketch.

Denote the wetted part of the shell surface through σ and the liquid free surface as S_0. The liquid volume is divided here into two domains Ω_1 and Ω_2 by the surface $S_{baf} \cup S_{int}$, where S_{baf} is a baffle surface, S_{int} is an interface surface (Biswal *et al.*, 1984), see Fig.1. The shell surface σ consists of four parts, $\sigma = S_{w1} \cup S_{w2} \cup S_{bot} \cup S_{baf}$. Here S_1 and S_2 are lateral surfaces of first and second fluid domains, respectively, and S_{bot} is a surface of the tank bottom.

Let $\mathbf{U} = (U_1, U_2, U_3)$ denote the vector-function of shell displacements. Consider at first stage the free vibrations of the shell without a liquid (the empty shell). For the problems of free vibrations we assume that the time dependent shell displacements are given by

$$\mathbf{U} = \mathbf{u}\exp(i\Omega t); \quad \mathbf{u} = (u_1, u_2, u_3)$$

Here Ω is the vibration frequency; the time factor $\exp(i\Omega)$ will be omitted further on. After the separation of the time factor, the vibrations of the shell without a liquid are described by the system of three partial differential equations

$$\sum_{i=1}^{3} L_{ij} u_i = \Omega^2 u_j, \quad j = 1,2,3,$$

where L_{ij} are linear differential operators of the Kirchhoff - Love shell theory Levitin et al. (Levitin & Vassiliev, 1996).

A finite element method was applied in (Ravnik *et al.*, 2016; Ventsel *et al.*, 2010) to evaluate the natural frequencies Ω_k and modes $\mathbf{u}_k$, $k = \overline{1, N}$ of the shell of revolution without a liquid. After forming the global stiffness **L** and mass **M** matrices, the following equation of motion for the shell containing fluid was obtained in (Ravnik *et al.*, 2016; Ventsel *et al.*, 2010):

$$\mathbf{LU} + \mathbf{M}\ddot{\mathbf{U}} = p_d \mathbf{n} + \mathbf{Q}, \tag{1}$$

where **n** is an external unit normal to the shell wetted surface, a term $p_d \mathbf{n}$ gives the fluid dynamical pressure upon the shell, normal to its surface, $\mathbf{Q} = \mathbf{Q}(t)$ is a vector of external load.

To model the fluid motion, a mathematical model has been developed based on the following hypotheses: the fluid is incompressible, the motion of the fluid is irrotational and inviscid, only small vibrations (linear theory) need to be considered. So a scalar velocity potential $\Phi(x,y,z,t)$ whose gradient represents the fluid velocity can be introduced.

The fluid pressure $p = p(x, y, z, t)$ acting on the wetted shell surface is obtained from the linearized Bernoulli's equation for a potential flow, Lamb (Lamb, 1993).

$$p = -\rho_l \left(\frac{\partial \Phi}{\partial t} + gz \right) + p_0; \quad p_s = -\rho_l g z; \quad p_d = -\rho_l \frac{\partial \Phi}{\partial t},$$

where g is the gravity acceleration, z is the vertical coordinate of a point in the liquid, ρ_l is the liquid density, p_s and p_d are static and dynamic components of the fluid pressure, p_0 is for atmospheric pressure.

Assuming the flow to be inviscid and irrotational, the incompressible fluid motion in the 3D tank is described by the Laplace equation for the velocity potential Φ

$$\nabla^2 \Phi = 0. \tag{2}$$

To determine this potential a mixed boundary value problem for the Laplace equation is formulated in the double domain $\Omega_1 \cup \Omega_2$ (Fig. 2). The non-penetration condition on the wetted tank surfaces σ is following [56]:

$$\left. \frac{\partial \Phi}{\partial \mathbf{n}} \right|_{\sigma} = \frac{\partial w}{\partial t}, \qquad w = (\mathbf{U}, \mathbf{n}). \tag{3}$$

Let function $\zeta(t, x, y)$ be the free surface elevation. The kinematics and dynamic boundary conditions on S_0 can be expressed as follows (Gnitko *et al.*, 2016):

$$\left. \frac{\partial \Phi}{\partial \mathbf{n}} \right|_{S_0} = \frac{\partial \zeta}{\partial t}; \quad p - p_0 \big|_{S_0} = 0. \tag{4}$$

To apply the multi-domain approach we divide the fluid domain into two sub-domains Ω_1 and Ω_2, shown in Fig. 2. Here we introduce the artificial interface surface S_{int}. Let $\sigma_1 = S_1 \cup S_{\text{bot}} \cup S_{\text{baf}}$ and $\sigma_2 = S_2 \cup S_{\text{baf}}$ are the shell surfaces contacting with a liquid in sub-domains Ω_1 and Ω_2. Then boundaries of sub-domains Ω_1 and Ω_2 are $\Sigma_1 = \sigma_1 \cup S_{\text{int}}$ and $\Sigma_2 = \sigma_2 \cup S_0$.

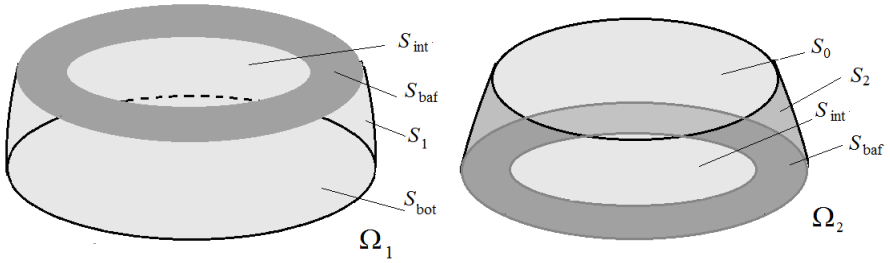

a) b)

Figure 2. Fluid sub-domains

Denote by φ_1, φ_2, φ_0 the potential values in nodes of σ_1, σ_2 and S_0, respectively. The fluxes on σ_1, σ_2 are known from the no-penetration boundary condition as w_1, w_2, and on the free surface the unknown flux is denoted as q_0. The potential and flux values on the interface surface S_{int} will be unknown functions φ_{ji} and q_j, $S_{\text{int}} \subset \Sigma_j$, $j = 1,2$, and we have (Brebbia *et.al.*, 1984)

$$\varphi_{2i} = \varphi_{1i}; \quad q_1 = -q_2 \tag{5}$$

Equations (1), (2) are solved simultaneously using the shell fixation conditions relative to **U**, boundary conditions (3)-(5), relative to Φ and the following expressions for the dynamical component of the liquid pressure on elastic walls:

$$p_d = (\mathbf{P}, \mathbf{n}) = -\rho_l \frac{\partial \Phi}{\partial t}.$$

To define modes of free harmonic shell vibrations coupled with liquid sloshing, we represent displacements of the fluid-filled tank as $\mathbf{U}=\mathbf{u_f}\cdot\exp(i\omega t)$. Here ω and $\mathbf{u_f}$ are natural frequencies and vibration modes of the fluid-filled shell structure.

3. The mode superposition method for coupled dynamic problems

Consider the vibration modes of the fluid-filled tank in a form

$$\mathbf{U} = \sum_{k=1}^{N} c_k \mathbf{u}_k , \tag{6}$$

where $c_k = c_k(t)$ are unknown coefficients, and $\mathbf{u}_k$ are eigenmodes of the empty tank. In other words, the mode of vibration of the fluid-filled tank is determined as a linear combination of eigenmodes of the empty shell structure. Note that the following relationships are fulfilled (Ventsel *et.al.*, 2010):

$$\mathbf{L}(\mathbf{u}_k) = \Omega_k^2 \mathbf{M}(\mathbf{u}_k), \quad (\mathbf{M}(\mathbf{u}_k), \mathbf{u}_j) = \delta_{kj} . \tag{7}$$

Hence

$$(\mathbf{L}(\mathbf{u}_k), \mathbf{u}_j) = \Omega_k^2 \delta_{kj} , \tag{8}$$

where Ω_k is the *k*-th frequency of the empty tank vibrations. Equations (7), (8) show that the abovementioned vibration modes have to be orthonormalized with respect to the mass matrix.

Consider the potential Φ as a sum of two potentials $\Phi = \Phi_1 + \Phi_2$, as it was done by Degtyarev et al in (Degtyarev *et al*.,2015).

The series for potential Φ_1 can be written as

$$\Phi_1 = \sum_{k=1}^{N} \dot{c}_k(t)\varphi_{1k} .$$

Here time-dependant coefficients $c_k(t)$ are defined in equation (6). To determine functions φ_{1k} the following boundary value problems are formulated:

$$\Delta\varphi_{1k} = 0, \left.\frac{\partial\varphi_{1k}}{\partial\mathbf{n}}\right|_{\sigma} = w_k, \ \varphi_{1k}\big|_{S_0} = 0, w_k = (\mathbf{u}_k, \mathbf{n}), \ k = \overline{1,N} \tag{9}$$

The solution of boundary value problems (9) was done by Ventsel et al in (Venstel *et al*., 2010). Thus the dynamic analysis of elastic shells of revolution with a liquid, neglecting the gravity force, is formulated in terms of the functions **U** and Φ_1. The above functions satisfy the system of differential equations (1), (2) the no-penetration condition and the lack of the pressure on a free surface, as well as the conditions of the shell fixation. The solutions of the boundary value problems (9) can be represented in the symbolic form as $\varphi_{1k} = i\Omega\mathbf{H}(\mathbf{u}_k)$, where $\mathbf{H}(\mathbf{u}_k)$ is the inverse operator of the hydrodynamic problem (Ventsel *et.al*., 2010).

Suppose that $c_k(t) = C_k \exp(i\omega t)$, where ω is an own frequency of the shell with a fluid. Based on the equations (1), (2), (9) we obtain

$$\left(\Omega_k^2\delta_{kj} + \delta_{kj}\right)C_j = \omega^2\rho_l\sum_{k=1}^{N} C_k\left(\mathbf{H}(\mathbf{u}_k), \mathbf{u}_j\right). \tag{10}$$

The above equation represents a generalized eigenvalue problem. Solving this problem yields the natural frequencies ω of the vibrations of the elastic shell conveying fluid, but without the gravity effects.

When the potential Φ_2 is known, the low frequency sloshing modes will be obtained. To determine the potential Φ_2 we have a problem of fluid vibrations in a rigid shell including gravity effects.

Use the expansion $\Phi_2 = \sum_{k=1}^{M} \dot{d}_k(t)\varphi_{2k}$, where $d_k.(t)$ are unknown coefficients, functions φ_{2k} are natural modes of the liquid sloshing in the rigid tank. To obtain these modes the following boundary value problems are considered:

$$\Delta\varphi_{2k} = 0; \qquad \left.\frac{\partial\varphi_{2k}}{\partial\mathbf{n}}\right|_{\sigma} = 0; \qquad \left.\frac{\partial\varphi_{2k}}{\partial t} + g\zeta\right|_{S_0} = 0; \ \left.\frac{\partial\varphi_{2k}}{\partial\mathbf{n}}\right|_{S_0} = \frac{\partial\zeta}{\partial t}, \ k = \overline{1,N} \tag{11}$$

The zero eigenvalue obviously exists for problem (11), but we exclude it with the help of the following orthogonality condition:

$$\iint_{S_0} \frac{\partial\varphi_{2k}}{\partial\mathbf{n}} dS_0 = 0$$

Differentiate the third equation in relationship (11) with respect to *t* and substitute there the expression for ζ_t' from the forth one of (11). Suppose

$\varphi_{2k}(t,x,y,z)=e^{i\chi_k t}\varphi_{2k}(x,y,z)$ and obtain the next conditions on the free surface for each mode φ_{2k} with the sloshing frequency χ_k:

$$\frac{\partial\varphi_{2k}}{\partial\mathbf{n}}=\frac{\chi_k^2}{g}\varphi_{2k},\quad k=1,M\,. \tag{12}$$

It leads to the following eigenvalue problems

$$\Delta\varphi_{2k}=0;\qquad \left.\frac{\partial\varphi_{2k}}{\partial\mathbf{n}}\right|_{\sigma}=0;\qquad \frac{\partial\varphi_{2k}}{\partial\mathbf{n}}=\frac{\chi_k^2}{g}\varphi_{2k},\ \iint\limits_{S_0}\varphi_{2k}dS_0=0,\quad k=\overline{1,M}\,. \tag{13}$$

Solving these problems yields the sloshing frequencies χ_k. and modes φ_{2k}.

So to solve the free vibration problem for an elastic shell of revolution coupled with liquid sloshing it is necessary to determine three systems of basic functions: modes of liquid in rigid shell under force of gravity; own modes of empty shell; modes of fluid-filled elastic shell without including the force of gravity.

Thus, the problem under consideration involves the following steps.

First, it is necessary to obtain the sloshing frequencies and modes φ_{2k} using rigid wall assumption.

Second, we obtain the natural frequencies Ω_k and modes $\mathbf{u}_k$ of the empty tank with elastic walls. It would be noted that the Kirchhoff-Love shell theory is employed here because of considering the thin shells, but for defining basic functions $\mathbf{u}_k$ one can involve another shell theory.

Then we define the free vibration frequencies and modes φ_{1k} of the elastic tank without considering effects of sloshing.

Finally, for the sum of potentials $\Phi=\Phi_1+\Phi_2$ the following expression can be written

$$\Phi=\sum_{k=1}^{N}\dot{c}_k(t)\varphi_{1k}+\sum_{k=1}^{M}\dot{d}_k(t)\varphi_{2k}\,. \tag{14}$$

The unknown function ζ takes the following form:

$$\zeta=\sum_{k=1}^{N}c_k(t)\frac{\partial\varphi_{1k}}{\partial n}+\sum_{k=1}^{M}d_k(t)\frac{\partial\varphi_{2k}}{\partial n}\,. \tag{15}$$

So, the total potential Φ satisfies the Laplace equation and non penetration boundary condition

$$\Delta\Phi=0;\ \left.\frac{\partial\Phi}{\partial\mathbf{n}}\right|_{S_1}=\frac{\partial w}{\partial t}$$

due to validity of relations (11),(13). Noted that Φ also satisfies the condition

$$\left.\frac{\partial\Phi}{\partial n}\right|_{S_0}=\frac{\partial\zeta}{\partial t}$$

as a result of representation (15).

Satisfying the condition

$$\left.\frac{\partial\Phi}{\partial t}+gz\right|_{s_0}=0$$

on the free surface, one can obtain the next equality

$$\sum_{k=1}^{N}\ddot{c}_k\varphi_{1k}+\sum_{k=1}^{M}\ddot{d}_k\varphi_{2k}+g\left(\sum_{k=1}^{N}c_k\frac{\partial\varphi_{1k}}{\partial z}+\sum_{k=1}^{M}d_k\frac{\partial\varphi_{2k}}{\partial z}\right)=0.$$

When functions φ_{1k} and φ_{2k} are defined, we substitute them in eqns (1),(4) and obtain the system of ordinary differential equations as it was done in (Gnitko *et al*., 2017).

$$L\left(\sum_{k=1}^{N}c_k(t)\mathbf{u}_k\right)+M\left(\sum_{k=1}^{N}\ddot{c}_k(t)\mathbf{u}_k\right)=-\rho_l\left(\sum_{k=1}^{N}\ddot{c}_k(t)\varphi_{1k}+\sum_{k=1}^{M}\ddot{d}_k(t)\varphi_{2k}\right);. \tag{16}$$

$$\sum_{k=1}^{M}\ddot{d}_k\varphi_{2k}+g\sum_{k=1}^{N}c_k\frac{\partial\varphi_{1k}}{\partial n}+\sum_{k=1}^{M}d_k\chi_k^2\varphi_{2k}=0.$$

The first equation here is valid on the wetted surface of the shell and the second one – on the free surface of liquid.

Considering the result of dot product of first equation in (16) by u_j and second one by φ_{2j}, taking also into account relationships (7),(8) and orthogonality of natural modes of fluid vibrations in rigid vessel, we come to the next set of *N*+*M* second order differential equations to determine unknown coefficients $c_k(t), d_k(t)$:

$$c_j(t)\Omega_j^2+\ddot{c}_j(t)=-\rho_l\left(\sum_{k=1}^{N}\ddot{c}_k(t)\left(\varphi_{1k},w_j\right)+\sum_{k=1}^{M}\ddot{d}_k(t)\left(\varphi_{2k},w_j\right)\right) \tag{17}$$

$$\ddot{d}_j(t)+g\sum_{k=1}^{N}c_k(t)\left(\frac{\partial\varphi_{1k}}{\partial n},\varphi_{2j}\right)+g\chi_j^2d_j(t)=0$$

To define coupled modes of harmonic vibrations we represent the time-dependant unknown coefficients as

$$c_k(t)=C_ke^{i\omega t};\quad d_k(t)=D_ke^{i\omega t}, \tag{18}$$

where ω is an own frequency, and C_k, D_k are unknown constants.

Taking into account equations (18), one can obtain that equations (17) can be expressed as

$$C_j\Omega_j^2-\omega^2C_j+\rho_l\left(\omega^2\sum_{k=1}^{N}C_k\left(\varphi_{1k},w_j\right)+\omega^2\sum_{k=1}^{M}D_k\left(\varphi_{2k},w_j\right)\right)=0,\quad j=\overline{1,N} \tag{19}$$

$$\chi_l^2D_l-\omega^2D_l+g\sum_{k=1}^{m}C_k\left(\frac{\partial\varphi_{1k}}{\partial n},\varphi_{2l}\right)=0,\quad l=\overline{1,M}.$$

Introducing the following matrixes and vectors

$$C=\begin{pmatrix}C_1\\C_2\\...\\C_m\end{pmatrix};\quad D=\begin{pmatrix}D_1\\D_2\\...\\D_n\end{pmatrix};\ H_\chi=\begin{pmatrix}\chi_1^2&.0&0\\0&...&...\\0&0&\chi_n^2\end{pmatrix};\ H_\omega=\begin{pmatrix}\Omega_1^2&.0&0\\0&...&...\\0&0&\Omega_m^2\end{pmatrix};$$

$$P=\{p_{kj}\};\quad p_{kj}=\left(\varphi_{1k},w_j\right);\quad k,j=\overline{1,N};$$

$$B=\{b_{jk}\};\quad b_{jk}=\left(\varphi_{2j},w_k\right);\ A=\{a_{jk}\};\quad a_{jk}=\left(\frac{\partial\varphi_{1k}}{\partial n},\varphi_{2j}\right);\quad k=\overline{1,N};\ j=\overline{1,M},$$

we come to the next eigenvalue problem

$$\omega^2EC+H_\omega C+\omega^2\rho_lPC+\omega^2\rho_lBD=0;$$

$$\omega^2ED+gAC+H_\chi D=0.$$

Let also introduce for simplicity vectors and matrix of doubled dimension $N+M$

$$X=\begin{pmatrix} C \\ D \end{pmatrix};\ H=\begin{pmatrix} E+\rho_2 P & \rho_2 B \\ 0 & E \end{pmatrix};\qquad G=\begin{pmatrix} H_\omega & 0 \\ gA & H_\chi \end{pmatrix}.$$

It brings us to the following eigenvalue problem

$$\left(G-\omega^2 H\right)X=0. \tag{20}$$

So free vibration analysis of an elastic shell coupled with liquid sloshing is reduced to the solution of generalized eigenvalue problem (20) where both elasticity and gravity effects are taken into account (Degtyarev *et al.*, 2015). It would be noted that hereinbefore we did not assume that the shell considered is a shell of revolution only. The effective numerical procedure for solution of this eigenvalue problems using the single and multi-domain boundary element methods (BEM) has been developed in (Gnitko *et al*., 2016; Ravnik *et al*., 2016).

4. Reducing to the system of one-dimensional integral equations

To define functions φ_{1k} and φ_{2k} we use the boundary element method in its direct formulation (Brebbia *et al*., 1984). Dropping indices 1*k* and 2*k* one can obtain the main integral equation in the following form

$$2\pi\varphi(P_0)=\iint\limits_S q\frac{1}{|P-P_0|}dS-\iint\limits_S \varphi\frac{\partial}{\partial\mathbf{n}}\frac{1}{|P-P_0|}dS. \tag{21}$$

Here $S=\sigma\cup S_0$, points P and P_0 belong to the surface S. The value $|P-P_0|$ represents Cartesian distance between the points P and P_0. In doing so, the function φ defined on the wetted tank surface σ presents the pressure, and the function q defined on the free surface S_0, is the flux, $q=\partial\varphi/\partial\mathbf{n}$.

The basic procedure is to start with the standard boundary integral equation for potential (21), replace Cartesian coordinates (x, y, z) with cylindrical ones (r, θ, z), and integrate with respect to θ, taking into account that

$$|P-P_0|=\sqrt{r^2+r_0^2+(z-z_0)^2-2rr_0\cos(\theta-\theta_0)},$$

where points P and P_0 have the following coordinates

$$P=(r,z,\theta);\quad P_0=(r_0,z_0,\theta_0).$$

Furthermore we represent unknown functions as Fourier series by the circumferential coordinate θ

$$w_k^i(r,z,\theta)=w_k^i(r,z)\cos\alpha\theta;\ \varphi_{jk}^i(r,z,\theta)=\varphi_{jk}^i(r,z)\cos\alpha\theta;\ i=1,2;\ j=1,2;\ k=1,2,\ldots, \tag{22}$$

where α is a given integer (the number of nodal diameters). In this case, the solution is independent of the angular coordinate θ, and the three-dimensional problem is reduced to a two-dimensional one in the radial coordinate r and the axial coordinate z.

Let Γ be a generator of the surface σ. Using (21), (22) we have obtained the following system of singular integral equations for unknown functions φ and q in problem (9):

$$2\pi\varphi(z_0)+\int_\Gamma \varphi(z)Q(z,z_0)r(z)d\Gamma-\int_0^R q(\rho)\Psi(P,P_0)\rho d\rho=\int_\Gamma w(z)\Psi(P,P_0)r(z)d\Gamma_1;P_0\in\sigma;$$

$$\int_\Gamma \varphi(z)Q(z,z_0)r(z)d\Gamma-\int_0^R q(\rho)\Psi(P,P_0)\rho d\rho=\int_\Gamma w(z)\Psi(P,P_0)r(z)d\Gamma_1;\ P_0\in S_0.\quad(23)$$

Here

$$Q(z,z_0)=\frac{4}{\sqrt{a+b}}\left\{\frac{1}{2r}\left[\frac{r^2-r_0^2+(z_0-z)^2}{a-b}\mathsf{E}_\alpha(k)-\mathsf{F}_\alpha(k)\right]n_r+\frac{z_0-z}{a-b}\mathsf{E}_\alpha(k)n_z\right\};$$

$$\Psi(P,P_0)=\frac{4}{\sqrt{a+b}}\mathsf{F}_\alpha(k);\ \mathsf{E}_\alpha(k)=(-1)^\alpha\left(1-4\alpha^2\right)\int_0^{\pi/2}\cos 2\alpha\psi\sqrt{1-k^2\sin^2\psi}\,d\psi;$$

$$\mathsf{F}_\alpha(k)=(-1)^\alpha\int_0^{\pi/2}\frac{\cos 2\alpha\psi d\psi}{\sqrt{1-k^2\sin^2\psi}};\ a=\rho^2+\rho_0^2+(z-z_0)^2;\quad b=2\rho\rho_0;\ k^2=\frac{2b}{a+b}.$$

Letting $\alpha=0$ in expressions (23), we obtain the standard elliptic first and second kind integrals.

The system of singular integral equations for mixed boundary value problems (11) has been obtained in (Gnitko *et al*., 2016).

To define potentials Φ_2 we introduce as in (Gnitko *et al*., 2016) next integral operators:

$$A\psi_1=2\pi\psi_1+\iint_{S_1}\psi_1\frac{\partial}{\partial n}\frac{1}{r(P,P_0)}dS_1;\ B\psi_0=\iint_{S_0}\psi_0\frac{1}{r}dS_0;$$

$$C\psi_0=\iint_{S_0}\psi_0\frac{\partial}{\partial z}\left(\frac{1}{r}\right)dS_0;\ D\psi_1=-\iint_{S_1}\psi_1\frac{\partial}{\partial n}\frac{1}{|P-P_0|}dS_1;\ F\psi_0=\iint_{S_0}\psi_0\frac{1}{r}dS_0.$$

Then the boundary value problem (13) takes the form

$$A\psi_1=(\chi^2/g)B\psi_0-C\psi_0;\ P_0\in S_1;\ D\psi_1=2\pi E\psi_0-(\chi^2/g)F\psi_0;\ P_0\in S_0.$$

After excluding function ψ_1 from these relations, we obtain the eigenvalue problem and its solution gives natural modes and frequencies of liquid sloshing in the rigid tank

$$(DA^{-1}C+E)\psi_0-\lambda(DA^{-1}B+F)\psi_0=0;\quad \lambda=\chi^2/g.$$

It should be noted that there are two types of kernels in the integral operators introduced above, namely

$$A(S,\sigma)\psi=\iint_S\psi\frac{\partial}{\partial\mathbf{n}}\frac{1}{|P-P_0|}dS;\quad B(S,\sigma)\psi=\iint_S\psi\frac{1}{|P-P_0|}dS;\quad P_0\in\sigma.\quad(24)$$

At integration with respect to θ one can conclude that the internal integrals in (24) are complete elliptic integrals of first and second kinds. As the first kind elliptic integrals are non-singular, one can successfully use standard Gaussian quadratures for their numerical evaluation. For second kind elliptic integrals we have applied here the approach based on the characteristic property of the arithmetic geometric mean AGM (*a*,*b*) (see Cox David, 1984). The above-mentioned characteristic property consists in following:

$$\int_0^{\frac{\pi}{2}} \frac{d\theta}{\sqrt{a^2\cos^2\theta + b^2\sin^2\theta}} = \frac{\pi}{2AGM(a,b)}.$$

To define $AGM(a,b)$ there exist the simple Gaussian algorithm, described below

$$a_0 = a; \quad b_0 = b; \; a_1 = \frac{a_0 + b_0}{2}; \quad b_1 = \sqrt{a_0 b_0}; \ldots a_{n+1} = \frac{a_n + b_n}{2}; \quad b_{n+1} = \sqrt{a_n b_n}; \ldots$$

$$AGM(a,b) = \lim_{n\to\infty} a_n = \lim_{n\to\infty} b_n. \tag{25}$$

It is a very effective method to evaluate the elliptic integrals of the second kind. Convergence $\varepsilon = |a_n - b_n| < 10^{-8}$ is achieved after 6 iterations (namely, $n = 6$ in (25)).

So we have the effective numerical procedures for evaluation of inner integrals, but integral equations (23) involve external integrals of logarithmic singularities and thus the numerical treatment of these integrals will also have to take into account the presence of this integrable singularity. Here integrands are distributed strongly non-uniformly over the element and standard integration quadratures fail in accuracy. So we treat these integrals numerically by special Gauss quadratures (Brebbia *et al.*, 1984) and applying technique proposed in (Naumenko & Strelnikova, 2002).

The solution of system (23) is independent of the angular coordinate θ, and the three-dimensional problem is reduced to a two-dimensional one in the radial coordinate r and the axial coordinate z. Using dependence $z = z(r)$, we finally reduce the system of singular integral equations to a one-dimensional one.

So 3-D problem of determining the pressure and free surface elevation is reduced to solution of the one-dimensional system of singular integral equations.

5. Multi-domain approach

To estimate the liquid vibrations in the presence of the baffle, we use the multi-domain method (boundary super-elements). In doing so, we introduce an "artificial" interface surface S_{int} (Brebbia *et al.*, 1984; Gnitko *et al.*, 2016; Gnitko *et al.*, 2017), divide the region filled with the liquid into two parts $\Omega_1; \Omega_2$, bounded by surfaces S_{bot}, S_1, S_{baf}, S_{int} and S_2, S_{baf}, S_{int}, S_0 and shown in Fig. 2. Let $\sigma_1 = S_1 \cup S_{\text{bot}} \cup S_{\text{baf}}$ and $\sigma_2 = S_2 \cup S_{\text{baf}}$ are the surfaces of the shell contacting with a liquid in sub-domains Ω_1 and Ω_2. Then boundaries of sub-domains Ω_1 and Ω_2 are $\Sigma_1 = \sigma_1 \cup S_{\text{int}}$ and $\Sigma_2 = \sigma_2 \cup S_0$. Denote by φ_1, φ_2, φ_0 the potential values in nodes of σ_1, σ_2 and S_0, respectively, and by w_1 , w_2 the values of function $w = (\mathbf{U}, \mathbf{n})$. The fluxes on σ_1, σ_2 are known from the no-penetration boundary condition as w_1, w_2 and on the free surface the unknown flux is denoted as q_0. The potential and flux values on the interface surface S_{int} will be unknown functions φ_{ji} and q_j, $S_{\text{int}} \subset \Sigma_j$, $j = 1,2$, and we have the following compatibility conditions

$$\varphi_{2i} = \varphi_{1i}; \quad q_1 = -q_2. \tag{26}$$

Consider the boundary value problem for determining the potential Φ_1. Introducing $\widetilde{S}_1 = \sigma_1$, $\widetilde{S}_2 = S_{\text{int}}$, $\widetilde{S}_3 = \sigma_2$, $\widetilde{S}_4 = S_0$ allows us to obtain matrixes $A_{ij} = A(\widetilde{S}_i, \widetilde{S}_j)$; $B_{ij} = B(\widetilde{S}_i, \widetilde{S}_j)$, $i, j = \overline{1,4}$. By using the multi-domain approach to determine the potential Φ_1 the next system of integral equations in the operator form was obtained in (Gnitko *et al*., 2017):

$$\begin{aligned}
&A_{11}\varphi_1 + A_{12}\varphi_{1i} = B_{11}w_1 + B_{12}q_1; \quad P_0 \in \sigma_1;\\
&A_{21}\varphi_1 + A_{22}\varphi_{1i} = B_{21}w_1 + B_{22}q_1; \quad P_0 \in S_{\text{int}};\\
&A_{32}\varphi_{1i} + A_{33}\varphi_2 = B_{33}w_2 - B_{32}q_1 + B_{34}q_0; \quad P_0 \in \sigma_2;\\
&A_{22}\varphi_{1i} + A_{23}\varphi_2 = B_{23}w_2 - B_{22}q_1 + B_{24}q_0; \quad P_0 \in S_{\text{int}};\\
&A_{42}\varphi_{1i} + A_{43}\varphi_2 = B_{43}w_2 - B_{42}q_1 + B_{44}q_0; \quad P_0 \in S_0.
\end{aligned} \tag{27}$$

It would be noted that compatibility conditions (26) are taking into account in system (27). As a result of solving equations (27), we have

$$\boldsymbol{\varphi} = \mathbf{Q}\mathbf{w}, \qquad \boldsymbol{\varphi} = \{\varphi_i\}_{i=1}^2; \mathbf{w} = \{w_i\}_{i=1}^2; \quad \mathbf{Q} = \{Q_{ij}\}_{i,j=1}^2,$$

where Q_{ij} are obtained in [26]. So for each φ_{1k} the pressure on the surface σ will be defined by formulae

$$p_k = -\rho_l \ddot{c}_k(t)\varphi_{1k}^i(P); P \in S_1 \cup S_{\text{bot}} \cup S_2; \; p_k = -\rho_l \ddot{c}_k(t)\left[\varphi_{1k}^1(P) - \varphi_{1k}^2(P)\right]; P \in S_{\text{baf}}.$$

The boundary value problem for determining the potential Φ_2 with multi-domain BEM (MBEM) was solved by Gnitko et al in (Gnitko *et al.,* 2016).

Hereinafter the results of numerical simulation are described. In Section 6 the convergence of proposed method is shown. Sections 7-10 are devoted to liquid sloshing in rigid shells, Sections 11-12 present results of fluid-structure interaction including both sloshing and elasticity effects.

6. Comparing with analytical solution and convergence

As it was mentioned above, for vibration analysis of elastic shells it is necessary to determine three systems of basic functions. One of them is represented by free vibrations modes of the liquid in the rigid shell under the force of gravity. So the first stage of our research is connected with the liquid vibrations in the rigid shells. We consider here rigid spherical, cylindrical and conical shells with and without baffles. The initial 3D problem is reduced to solution of the one–dimensional system of singular integral equations in the form (23). In Fig. 3 the drafts of shells are shown with discretized geometry based on BEM.

In Fig. 3 the following designation are introduced: N_0 is the number of boundary elements along the free surface radius; N_{w} is the number of boundary elements along the shell wall; N_{inf} is the number of boundary elements along the interface surface; N_{baf} is the number of boundary elements along the baffle; and N_{bot} is the number of boundary elements along the shell bottom.

To validate the proposed method the rigid cylindrical is considered. The first set of calculations is therefore to determine the requisite number of boundary elements for a precise determination of the natural frequencies.

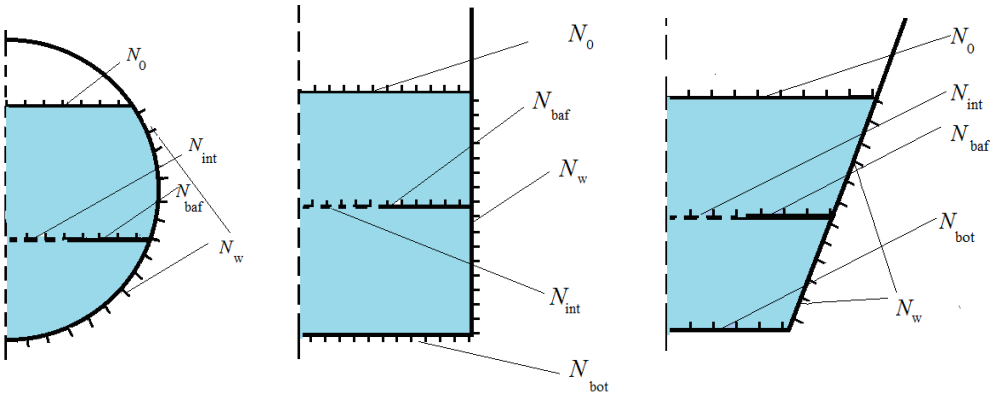

Figure 3. Drafts of shells and discretization

We consider liquid sloshing in the rigid cylindrical shell. For testifying the proposed numerical algorithm we use the analytical solution (Abramson, 2000) that can be expressed in the next form:

$$\frac{\chi_k^2}{g} = \frac{\mu_k}{R}\tanh\left(\mu_k \frac{H}{R}\right), k = 1,2,..; \varphi_{2k} = J_\alpha\left(\frac{\mu_k}{R} r\right)\cosh\left(\frac{\mu_k}{R} z\right)\cosh^{-1}\left(\frac{\mu_k}{R} H\right). \qquad (28)$$

Here R is the shell radius, H is its height, values μ_k are roots of the equation $J'_\alpha(x) = 0$, where $J_\alpha(x)$ is Bessel function of the first kind, χ_k, φ_{2k} are frequencies and modes of liquid sloshing in the rigid cylindrical shell. The numerical solution is obtained by using the BEM as it was described beforehand.

Consider the rigid circular cylindrical shell with a flat bottom, without baffles, and having the following parameters: the radius and height are R = 1 m, and H=1m. Table 1 below provides the numerical values of the natural frequencies of liquid sloshing for nodal diameters α =0 and α =1 obtained by proposed numerical method for different numbers N_0, N_w, and N_{bot} and analytical values received by formula (28). Here we choose equal numbers N_0 =N_w = N_{bot} because radii of the free surface and bottom, and the height of the wetted part of the are equals to 1m. So we consider the following sizes of one-dimensional boundary elements according to numbers N_0=N_w=N_{bot}: 0.04m; 0.02 m, and 0.01m.

Table 1. Slosh frequency parameters χ_n^2 / g of the fluid-filled rigid cylindrical shell

α	BEM			n=1	n=2	n=3	n=4	n=5
	N_0	N_w	N_{bot}					
0	25	25	25	3.8289	7.0163	10.1761	13.3152	6.47089
	50	50	50	3.8285	7.0159	10.1735	13.3243	6.47066
	100	100	100	3.8281	7.0156	10.1732	13.3233	6.47060
	Analytical solution			3.8281	7.0156	10.1734	13.3236	6.47063
1	N_0	N_w	N_{bot}	n=1	n=2	n=3	n=4	n=5
	25	25	25	1.6590	5.3301	8.5385	11.7071	14.8684
	50	50	50	1.6579	5.3297	8.5372	11.7082	14.8655
	100	100	100	1.6573	5.3293	8.5366	11.7066	14.8635
	Analytical solution			1.6573	5.3293	8.5363	11.7060	14.8635

The results of Table 1 testify convergence of proposed BEM. In should be noted that the accuracy $\varepsilon = 10^{-4}$ has been achieved here for $N_0 = N_w = N_{bot} = 100$. So further we consider boundary elements with length near 1% of the characteristic size.

In Fig. 4 the distributions of first three sloshing modes for $\alpha = 0$ on the free surface are shown. The solid lines denote modes obtained by analytical expression (28) at $z = H$. The lines pointed with circles and squares denote numerical solutions at $N_0 = N_w = N_{bot} = 100$.

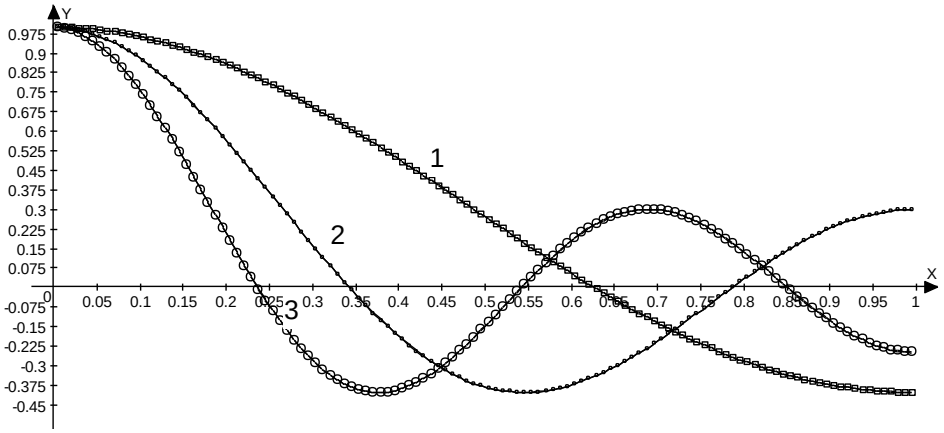

Figure 4. Numerically and analytically obtained modes

Fig. 4 also demonstrates good agreement between numerical and analytical data.

7. Cylindrical shells with and without baffles

The study of free vibration characteristics of the rigid cylindrical shell interacting with the liquid is presented here. It is supposed that α=0,1 in equation (22), i.e. we consider both axisymmetric and non- axisymmetric modes.

Consider the circular cylindrical shell with a flat bottom and having the following parameters: radius is R = 1 m, the thickness is h = 0.01 m, the length L = 2 m. The fluid filling level is denoted by H. The baffle is considered as a circle flat plate with a central hole (the ring baffle), fig. 5. The vertical coordinate of the baffle position (the baffle height) is denoted as H_1 ($H_1 < H$). The interface surface radius is denoted as R_{int} and we also have $H = H_1 + H_2$. So the baffle radius is $R_{baf} = R - R_{int}$.

The numerical solution is obtained by using the BEM as it is described beforehand. In present numerical simulation we used 100 boundary elements along the bottom (N_b), 120 elements along wetted cylindrical parts (N_w), and 100 elements along the radius of free surface (N_0). At the interface and baffle surfaces we used different numbers of elements depending on radius of the baffle. In numerical simulations we consider different values both for R_{int} and H_1. We used for comparison and validation the analytical solution (Ibrahim, 2005) that can be expressed by formulae (28).

To validate our multi-domain BEM approach we also have calculated the natural sloshing frequencies at H_1=0.5m, H_1=0.9m, and with R_{int}=0.7m, H=1.0m. The comparison of results obtained with proposed MBEM and the analytically oriented approach presented by I. Gavrilyuk *et al*. in (Gavrilyuk *et al*., 2008) is shown in Table 2.

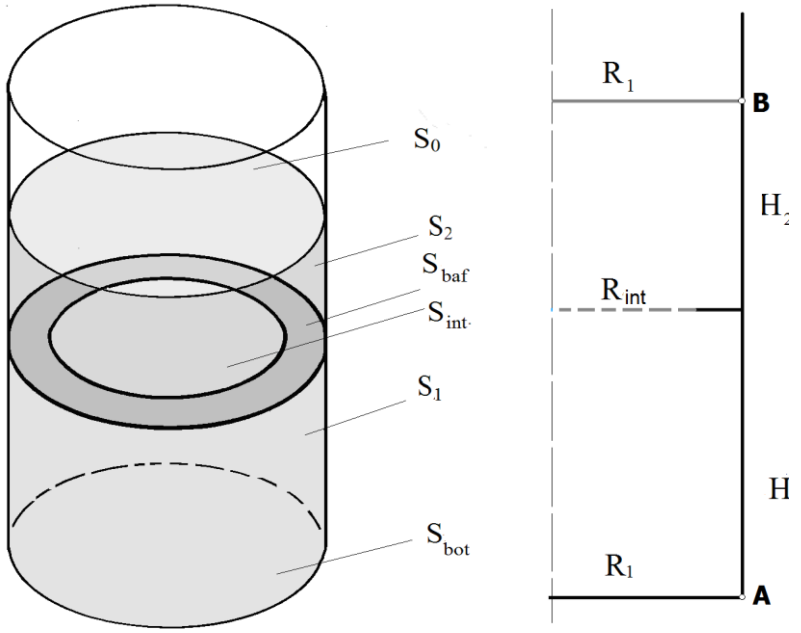

Figure 5. Cylindrical shell with internal baffle and its sketch

Table 2. Comparison of numerical results for $\omega^2 = \chi^2 / g$, α=0.

baffle position	method	*n*=1	*n*=2	*n*=3	*n*=4
H_1=0.5	MBEM	3.756	7.012	10.176	13.328
	(Gavrilyuk *et al.*, 2008)	3.759	7.010	10.173	13.324
H_1=0.9	MBEM	2.278	6.200	9.609	12.810
	(Gavrilyuk *et al.*, 2008)	2.286	6.197	9.608	12.808

These results have demonstrated a good agreement and validated the proposed multi-domain approach. In all tables we have compared the frequency parameters $\omega^2 = \chi^2 / g$ of the problems described beforehand.

The three first modes of liquid vibrations for α =0 are shown on Fig.6. Here we consider R_{int}=0.2m and the height of baffle installation H_1=0.9m.

Here numbers 1,2,3 correspond to the first, second and third sloshing modes. The combination of R_{int}=0.2m and H_1=0.9m brings to frequencies' maximal decreasing. From Figure 6 one can conclude that modes of vibrations of baffled and un-baffled tanks are similar, and numerical values do not differ significantly.

Consider α=1. In this case values μ_k are roots of the equation (see the handbook of I.S. Gradshteyn and I.M Ryzhik, (Gradshteyn & Ryzhik, 2000))

$$J_1'(x) = 2[J_0(x) - J_2(x)]. \tag{29}$$

Table 3 hereinafter provides the numerical values of the frequencies parameters of liquid sloshing for nodal diameters α =0 and H=1.0m. The numerical results obtained with proposed MBEM are compared with those received using formulae (20), (21).

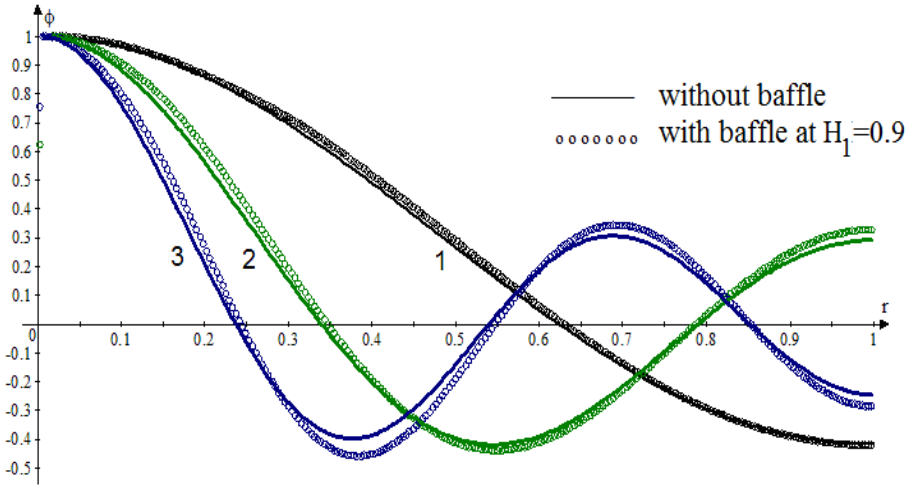

Figure 6. Modes of vibrations of un-baffled and baffled tanks

Table 3. Comparison of analytical and numerical results, α=1

Modes	*n*=1	*n*=2	*n*=3	*n*=4	*n*=5
MBEM	1.750	5.332	8.538	11.709	14.870
Analytical solution, (Gradshteyn & Ryzhik, 2000)	1.750	5.331	8.536	11.706	14.864

We also have calculated the natural sloshing frequencies for α=1 at H_1=0.5m, H_1= 0.9m, and with R_{int} =0.7m. The comparison of results obtained with proposed MBEM and the analytically oriented approach presented by I. Gavrilyuk et al (Gavrilyuk *et al.*, 2008) has been demonstrated in Table 4.

Table 4. Comparison of analytical and numerical results, α=1

Position	method	*n*=1	*n*=2	*n*=3	*n*=4
H_1=0.5	MBEM	1.3663	5.2941	8.5359	11.7097
	(Gavrilyuk *et al*., 2008)	1.3662	5.2940	8.5357	11.7092
H_1=0.9	MBEM	0.7078	4.5066	8.1947	11.5556
	(Gavrilyuk *et al*., 2008)	0.7079	4.5068	8.1945	11.5550

The three first modes of liquid vibrations are shown on Fig. 7. Here we consider the ring baffle with R_{int}=0.2m and the height of baffle installation H_1=0.9m.

Curves with numbers 1, 2, 3 correspond to the first, second, and third sloshing modes. These results demonstrate that modes of vibrations of baffled and un-baffled tanks at α=1 differ more significantly than those at α=0.

Results presented here may serve as the basis for designing liquid containers subjected to external excitations whose frequencies may be close to the lowest natural frequency of the free surface.

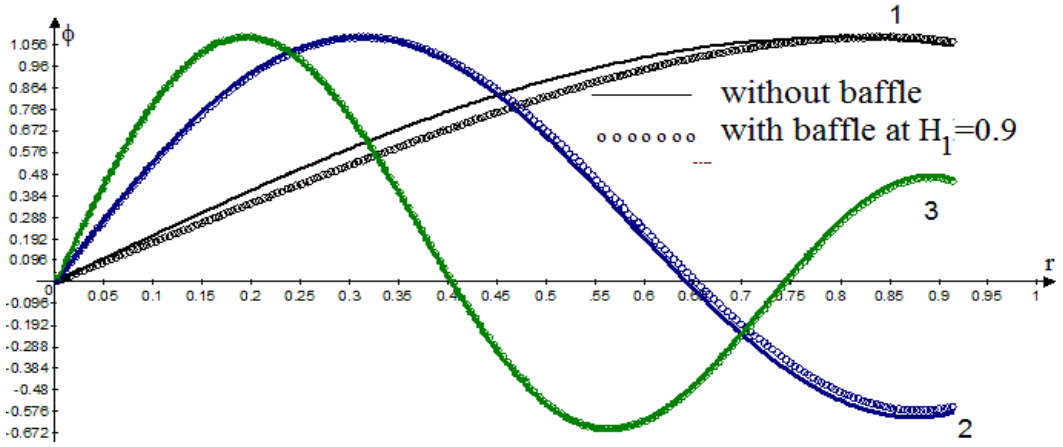

Figure 7. Modes of vibrations of un-baffled and baffled tanks, α=1

8. Conical shell with and without baffles

Conical shells in interaction with a fluid have received a little attention in scientific literature in spite of the usage of thin walled conical shells is of much importance in a number of different branches of engineering. In aerospace engineering such structures are used for aircraft and satellites. In ocean engineering, they are used for submarines, torpedoes, water-borne ballistic missiles and off-shore drilling rigs, while in civil engineering conical shells are used as containment vessels in elevated water tanks. The difficulty of using the analytical methods arises due to the fact that walls are not parallel to the axis of symmetry.

Boundary element method retains its advantages in this case.

We consider both V-shape and Λ-shape conical tanks with radius R_1=1.m, and θ=π/6, Fig. 8. Note, that for V-shape tank R_1 is the free surface radius, whereas for Λ-shape tank R_1 is radius of the bottom, and for V-shape tank R_2 is radius of bottom, where as for Λ-shape tank R_2 is the free surface radius.

If R_1, R_2 and θ are known quantities, than the corresponding value of H can be easy found as $H=(R_1-R_2)\cot\theta$.

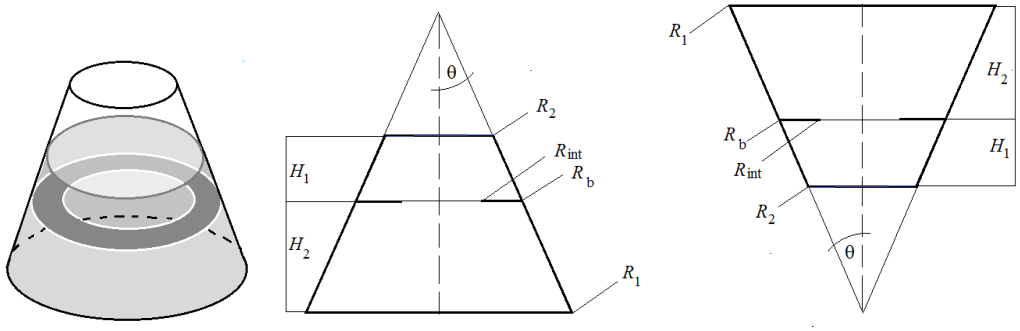

Figure 8. Baffled conical shells of Λ- and V shapes

In Table 5 the results of numerical simulation of the un-baffled tanks frequencies are presented for α =0, 1, 2 and different values of R_2. Our numerical simulation was dedicated to the frequencies $\omega_k^2 = \chi_k^2 / g$ for α =0, 1 ,2 and k =1 because these are the lowest natural frequencies that give the essential contribution to the hydrodynamic load.

Table 5. Frequency parameter $\omega_k^2 = \chi_k^2 / g$ of V – shape and Λ- – shape conical tanks

	V – shape					Λ – shape				
R_2	0.2	0.4	0.6	0.8	0.9	0.2	0.4	0.6	0.8	0.9
α =0, k =1										
(Gavrilyuk *et al*., 2008)	3.386	3.386	3.382	3.139	2.187	24.153	10.014	6.665	4.550	2.683
MBEM	3.389	3.390	3.391	3.192	2.200	20.027	10.034	6.669	4.545	2.678
α =1, k =1										
(Gavrilyuk *et al*., 2008)	1.304	1.302	1.254	0.934	0.542	11.332	5.629	3.515	1.661	0.726
MBEM	1.305	1.307	1.259	0.954	0.574	11.303	5.626	3.481	1.651	0.732
α =2, k =1										
(Gavrilyuk *et al*., 2008)	2.263	2.263	2.255	2.015	1.361	17.760	8.967	5.941	3.724	1.923
MBEM	2.265	2.270	2.269	2.048	1.394	17.939	8.965	5.941	3.726	1.951

The comparison of results obtained by proposed method with data of I. Gavrilyuk et al (Gavrilyuk *et al*., 2008) is presented here. The results are in good agreement except the data for Λ- shape tank with for α =0 and R_2=0.2m. But it was noted in (Gavrilyuk *et al*., 2008) that in this case the low convergence was achieved using the proposed there analytical method. Next, we have carried out the numerical simulation of the natural frequencies of liquid sloshing for tanks with baffles. Both V-shape and Λ-shape baffled tanks are under consideration. We consider tanks of height $H=H_1+H_2$=1.0m with different baffle positions H_1. We use R_1 = 1.0m and R_2=0.5.m for both type of tanks (see Fig. 8).

In Table 6 the results of numerical simulation are presented for α =0, 1 and different baffle positions, described by the height H_1. Here we consider four eigenvalues for α=0,1. Radius of the conical shell at the baffle position is denoted as R_b, and the free surface radius is R_{int} (Fig. 8). First, we have obtained the natural frequencies of V-shape and Λ-shape conical tanks without baffles. It corresponds to values H_1= H_2 =0.5m, R_{int}/R_b=1. The values of H_1 and H_2 can be arbitrary chosen, but H_1+H_2=1.0m. Then we have put baffles at the different positions H_1=0.5m and H_1=0.8m and considered the different sizes of baffles, namely R_{int}/R_b=0.5 and R_{int}/R_b=0.2.

The results obtained show different behaviour of decreasing frequencies for V-shape and Λ-shape conical tanks. For Λ-shape tanks the baffle positions and their sizes are not affected essentially on the values of frequencies. For V- shape tanks the effects of baffle characteristics is more considerable.

It would be noted also that the first harmonic frequencies are lower than axisymmetric ones both for V-shape and Λ-shape conical tanks.

The analytical numerical treatment for conical containers may require choosing a coordinate system where most of boundary conditions may be exactly satisfied. The

proposed BEM does not require any transformations of initial equations and involving the special coordinate system.

Table 6. Natural frequencies of V- shape and Λ-shape conical tanks with baffles

n			1	2	3	4	1	2	3	4
			V-shape				Λ-shape			
H_1	H_2	R_{int}/R_b	α =0							
0.5	0.5	1	3.466	6.681	9.845	12.99	7.985	14.37	20.70	27.01
0.5	0.5	0.5	3.408	6.668	9.843	12.99	7.968	14.37	20.69	27.01
0.5	0.5	0.2	3.405	6.635	9.843	12.99	7.960	14.37	20.69	27.01
0.8	0.2	0.5	2.527	6.387	9.724	12.92	7.344	14.25	20.66	26.99
0.8	0.2	0.2	2.443	6.059	9.565	12.88	7.113	14.20	20.65	26.99
			α =1							
0.5	0.5	1	1.416	4.997	8.206	11.37	4.424	11.09	17.46	23.79
0.5	0.5	0.5	1.228	4.974	8.197	11.37	4.192	11.06	17.46	23.79
0.5	0.5	0.2	1.172	4.943	8.196	11.37	4.037	11.06	17.45	23.79
0.8	0.2	0.5	0.815	4.742	8.003	11.20	3.128	10.78	17.42	23.77
0.8	0.2	0.2	0.630	4.191	7.849	11.23	2.529	10.66	17.36	23.75

9. Partially filled rigid spherical baffled and un-baffled shells

Spherical tanks partially filled with liquid are difficult to analyze the free-liquid natural frequencies and mode shapes using analytical methods. The difficulty arises due to the fact that walls are not straight. Liquid spattering and sloshing in spherical tanks was studied in papers (Faltinsen & Timokha, 2012; Kulczycki *et al.*, 2016). A characteristic feature of spherical tanks is the change in radius of a free surface with changing in a filling level. There exist known analytical solutions for almost completely filled tanks with small radii of the free surface, the so-called "ice fishing problems" formulation. The effect of baffles on sloshing frequencies was studied by Biswal *et al*. (Biswal *et al.*, 1984).

In this paper we consider the problem of fluid vibrations in the rigid spherical shells with and without baffles. To reduce the sloshing in the shell, an internal baffle is installed, Fig. 9.

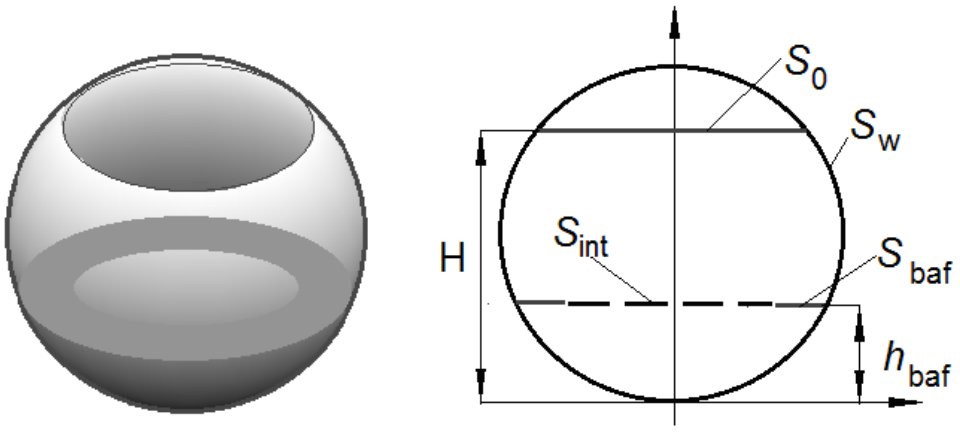

Figure 9. Spherical fuel tank with internal baffle

We denote here the wetted surface of the shell by $S_w = S_1 \cup S_2$, S_1 and S_2 are used when the baffled shell is under consideration.

Consider the spherical shell of radius R = 1 m, partially filled with the ideal

incompressible fluid, with the filling level *H*. Numerical analysis is carried out for $(0.2 < H/R < 1.99)$ and various $\alpha\,(\alpha = \overline{0,3})$.

Both single (SBEM) and multi-domain (MBEM) boundary element methods are applied here. The boundary elements with constant approximation of unknowns inside elements are used. In SBEM there are 200 elements along the spherical surface (N_w) and 150 elements along the free surface. In MBEM we divide the computational domain into two parts by the artificial interface surface at $h_{int} = 0.5H$ using 100 boundary elements in each sub-domain along the spherical surface and 150 elements along the free surface. We use practically the same mesh to find a numerical approximation of low eigenvalues for the so called "ice-fishing problem". In this problem, formally, we should consider an infinitely wide and deep ocean covered with ice, with a small round fishing hole. Sloshing in such "containers" was studied by McIver (McIver, 1989). We approximate this infinite case using the spherical tank with the very small round hole on its top. It allows us to compare our numerical results with those obtained in papers (Kulczycki *et al*., 2016; McIver, 1989).

In Tables 7-8 we compare our results obtained by using SBEM and MBEM with those obtained in (Kulczycki *et al*., 2016) – (McIver, 1989) for axisymmetric (α=0) and non-axisymmetric (α=1) modes. Four first frequencies ($m = \overline{1,4}$) are evaluated for each α. Here we consider different filling levels h_1. The value h_1/R_1=1.99 corresponds to the ice-fishing problem. Obtained results and results of Faltinsen et al (Faltinsen & Timokha, 2012) and Kulczycki et al. (Kulczycki *et al.*, 2016) are very close.

Different levels of fluid filling are considered, including *H/R* = 1.99, that corresponds to «ice-fishing problem», (McIver, 1989).

Table 7. Axisymmetric slosh frequencies parameters χ_n^2 / g of the fluid-filled spherical shell.

m	method	Filling level *H*, m				
		H =0.2	*H* =0.6	*H* =1.0	*H* =1.8	*H* =1.99
1	(Kulczycki *et al.*, 2016)	3.8261	3.6501	3.7451	6.7641	29.0500
	(Cho & Lee, 2004)	3.8261	3.6501	3.7451	6.7641	29.2151
	MBEM	3.4034	3.5455	3.7294	6.6098	30.7081
	SBEM	3.8314	3.6510	3.7456	6.7665	29.1811
2	(Kulczycki *et al*., 2016)	9.2561	7.2659	6.9763	12.1139	51.8122
	(McIver, 1989)	9.2561	7.2659	6.9763	12.1139	52.0467
	MBEM	9.2636	7.2893	6.9796	12.0008	52.9393
	SBEM	9.2686	7.2684	6.9780	12.1205	52.0255
3	(Kulczycki *et al.*, 2016)	14.7556	10.7443	10.1474	17.3960	74.2909
	(Cho & Lee, 2004)	14.7556	10.7443	10.1474	17.3960	74.5537
	MBEM	14.9214	10.7483	10.1496	17.3136	75.3139
	SBEM	14.7763	10.7502	10.1512	17.4086	74.5547
4	(Kulczycki *et al*., 2016)	20.1187	14.1964	13.3041	22.6579	96.6207
	(Cho & Lee, 2004)	20.1187	14.1964	13.3041	22.6570	96.9560
	MBEM	20.2066	14.2023	13.3083	22.5962	97.7771
	SBEM	20.1498	14.2056	13.3110	22.6777	96.9021

The results of calculations with SBEM and MBEM are close, in some cases SBEM gives more accuracy compared with MBEM, but the matrix size in SBEM is twice larger compared with MBEM. If un-baffled tanks are at low filling levels, it is preferable to use SBEM.

Table 8. Non-axisymmetric slosh frequencies parameters χ_n^2 / g of the fluid-filled spherical shell

m	method	Filling level *H*, m				
		H =0.2	*H* =0.6	*H* =1.0	*H* =1.8	*H* =1.99
1	(Kulczycki *et a* 2016),	1.0723	1.2625	1.5601	3.9593	18.9838
	(McIver, 1989)	1.0723	1.2625	1.5601	3.9593	19.1582
	MBEM	1.1034	1.2777	1.5638	3.9606	19.1603
	SBEM	1.0723	1.2626	1.5603	3.9508	19.1130
2	(Kulczycki *et a* 2016)	6.2008	5.3860	5.2755	9.4534	41.3491
	(McIver, 1989)	6.2008	5.3860	5.2755	9.4534	41.7683
	MBEM	6.1227	5.3534	5.2749	9.4582	41.5327
	SBEM	6.2090	5.3697	5.2764	9.4538	41.5333
3	(Kulczycki *et a* 2016)	11.8821	8.9418	8.5044	14.7548	63.5354
	(McIver, 1989)	11.8821	8.9418	8.5044	14.7548	64.0323
	MBEM	11.9650	8.9529	8.5062	14.7648	63.9483
	SBEM	11.8981	8.9429	8.5069	14.7574	63.8783
4	(Kulczycki *et a* 2016)	17.3581	12.4234	11.6835	20.0224	85.9166
	(McIver, 1989)	17.3584	12.4234	11.6835	20.0224	86.3001
	MBEM	17.4540	12.4276	11.6863	20.0394	86.2972
	SBEM	17.3842	12.4291	11.6884	20.0278	86.2034

From results of Tables 7-8 one can observe sloshing frequencies behaviour with increasing the fluid depth *H*. If radius R_0 of the free surface increases, then the frequencies decrease. In Table 9 the frequency parameters of axisymmetric sloshing are compared for cylindrical and spherical shells via different ratios H/R_0; where R_0 is radius for cylindrical shells. For defining the frequencies of cylindrical shells we use formulae (28).

Table 9. Axisymmetric slosh frequencies parameters χ_n^2 / g of the fluid-filled cylindrical and spherical shells

H, m	0.2	0.6	1.0	1.8	1.99
R_0	0.6	0.9165	1.0	0.6	0.1410
H/R_0	0.3333	0.6546	1.0	3.0	14.106
cylinder	5.4649	3.8959	3.8281	6.3861	27.1752
sphere	3.8261	3.6501	3.7451	6.7641	29.2151

Frequency changing of cylindrical shells has similar non-monotonic behaviour.

Fig.10 below demonstrates the spatial wave patterns for α=0, 1, *n*=1,2,3 at *H*=1.8m; *R*=1m.

Considering our approximate natural sloshing modes one can observe how free surface profiles change with the liquid depth.

These results are illustrated in Fig. 11 for the three lowest eigenvalues of the mode α = 0. Here numbers 1,2,3,4 correspond to the different filling levels, namely *H* =1.0m; 0.2m; 1.8m; 1.9m, respectively.

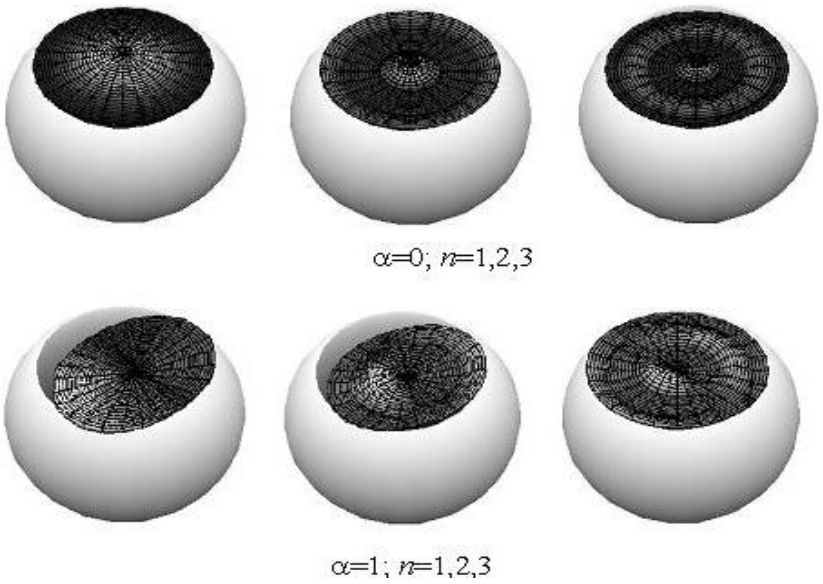

Figure 10. Spatial wave patterns for α=0,1

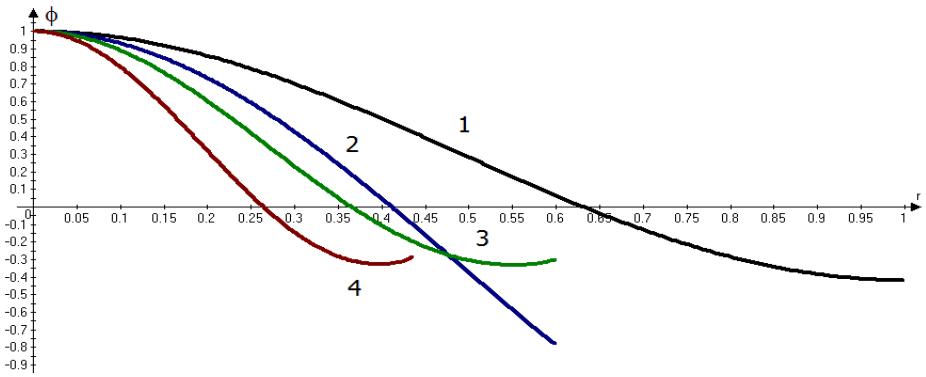

α = 0, *n*=1

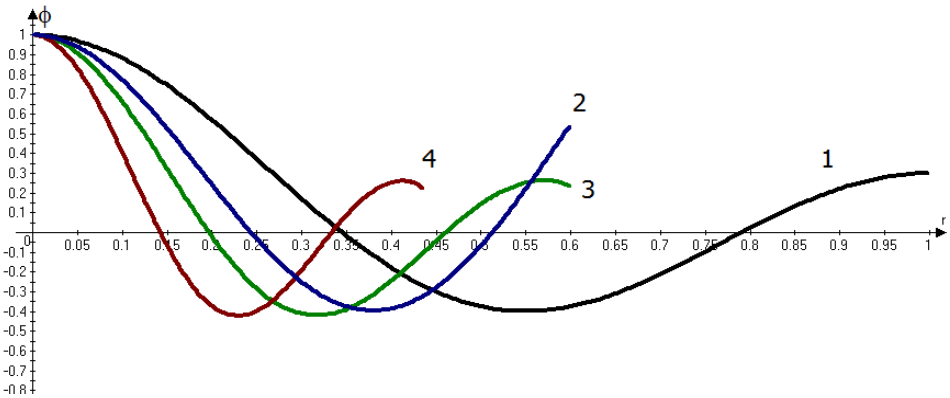

α = 0, *n*=2

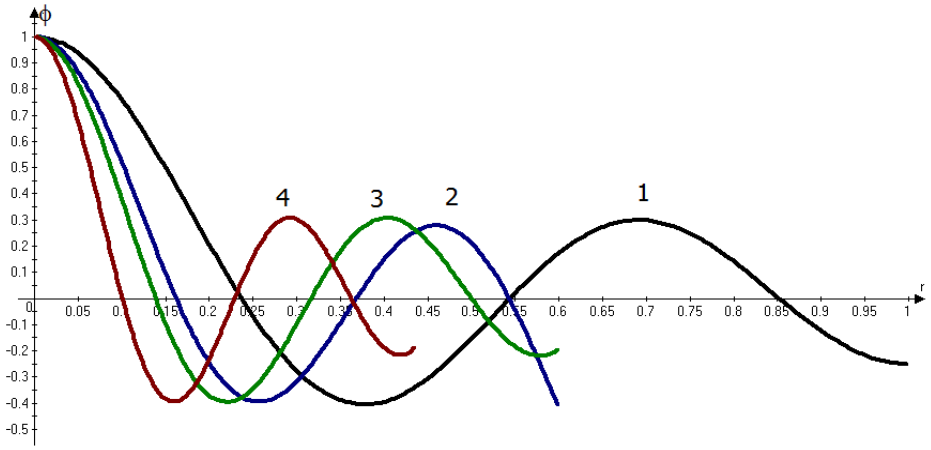

α = 0, *n*=3

Figure 11. The radial wave profiles α = 0, *m*=1,2,3, for different liquid depths *H*

We also consider non-axisymmetric modes, α = 1, because the frequencies corresponded to these modes are the lowest ones.

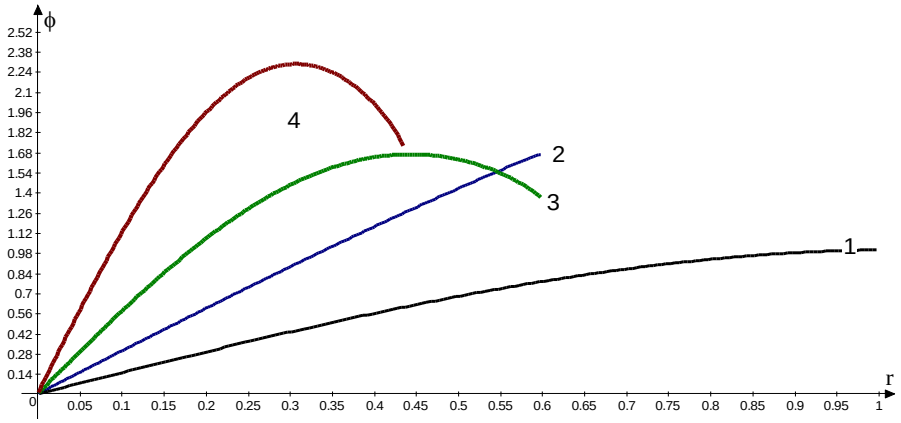

α = 1, *n*=1

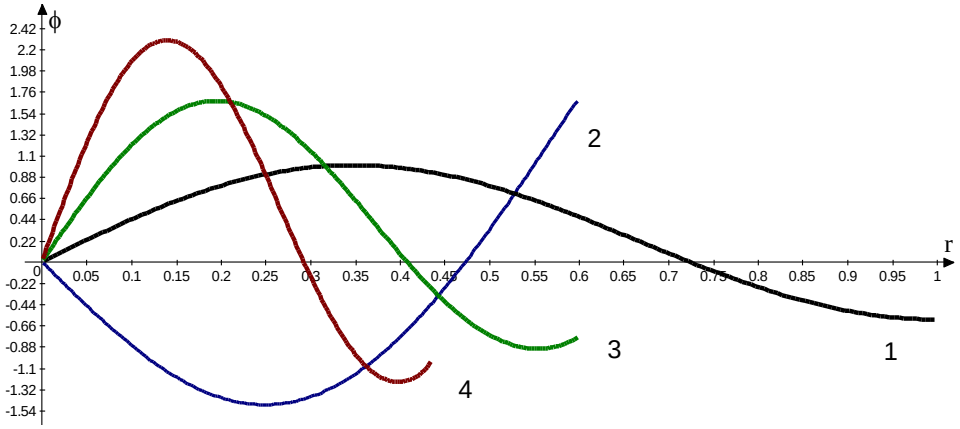

α = 1, *n*=2

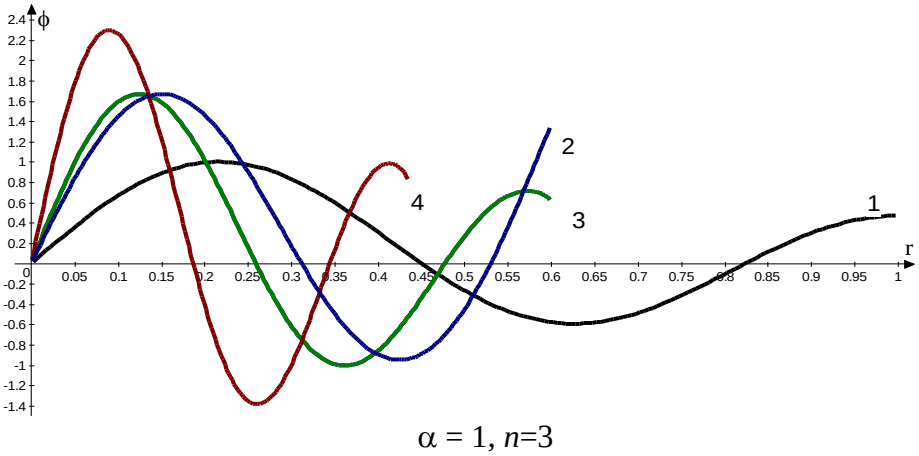

Figure 12. The radial wave profiles α = 1, *m*=1,2,3, for different liquid depths *H*

It would be noted that mode shapes presented in Fig. 12 have different magnitudes in their picks, because these modes are not normalized. There dividing by R_0 is applied for comparison with results O.M. Faltinsen and A.N. Timokha (Faltinsen & Timokha, 2012) where namely such non-normalized modes are presented.

In the spherical tank with $0 < H/R < 0.5$ the lowest mode presents a spatial wave pattern that look like inclination of an almost flat free surface. Increasing the liquid depth yields more complicated free surface profiles.

Next, the rigid spherical tank of radius R_1=1m filled to the depth H=1.4m is considered. The inner periphery of the tank contains a thin rigid-ring baffle. The baffle position is h_{baf}=1m. The different annular orifices in the baffle are considered. Radii of these orifices are radii R_{int} of the interface surfaces. The first three frequencies for mode α=1 are evaluated for radii R_{int} =1.0m, R_{int}=0.7m, and R_{int}=0.2m. Note that R_{int} =1.0m correspond to the un-baffled tank. These frequencies are presented in Table 5.

Table 10. Vibrations of the tank with a baffle, frequency parameter ω^2/g

m	ω^2/g		
	R_{int}=1.0 m	R_{int}=0.7m	R_{int}= 0.2 m
1	2.1232	2.0435	1.4234
2	5.9800	5.9723	5.8405
3	9.4789	9.4785	9.4567

Fig. 13 shows the first three forms of fluid vibrations in the spherical shell at α=1 with baffles.

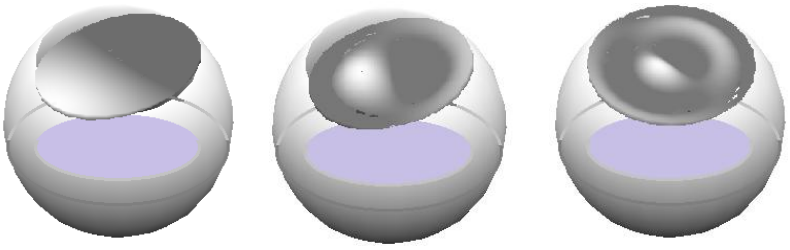

Figure 13. Modes of liquid vibrations in the baffled spherical shell.

When the baffle is installed, the mode shape becomes almost flat. The presence of the baffle has affected drastically only on the lower frequencies. Also one can see that small baffles (when R_{int} is relatively large) do not affect the lower frequencies.

10. Impulse impacts on reservoirs

Consider the rigid cylindrical shell with the flat bottom partially filled with the liquid. The tank parameters are following: radius is R = 1 m, thickness is h=0.01m, length is L = 2 m, filling level is H =1.0m.

We determine pressure p upon shell walls from the linearized Cauchy-Lagrange's integral by the following formula (Lamb, 1993):

$$p = -\rho_l\left(\Phi'_t + gz\right) + p_0 + a_s(t)x\,,$$

Here $a_s(t)$ is a function characterizing external influence (a horizontal seism or an impulse). The radial load is suddenly applied to cylindrical surface of the tank $a_s(t) = Q_0 a(t)$, where Q_0 = 10 MPa – distributed pressure,

$$a(t) = \begin{cases} 1, & t < T \\ 0, & t \geq T \end{cases}, \quad T = \text{ 1.5 s.}$$

Having defined the basic functions φ_{2k}, substitute them in expressions for velocity potential

$$\Phi = \sum_{k=1}^{M} \dot{d}_k \varphi_{2k}$$

and for the free surface elevation

$$\zeta = \sum_{k=1}^{M} d_k(t) \frac{\partial \varphi_{2k}}{\partial n} \tag{30}$$

Then substitute the received relations in the boundary condition on the free surface

$$\Phi'_t + g\zeta + a_s(t)x\big|_{s_0} = 0\,. \tag{31}$$

As in cylindrical system of coordinates there is $x = r\cos\theta$, we will be interested only in the first harmonica, i.e. in a formula (22) we only consider α=1. We come to the following equation on the surface S_0

$$\sum_{k=1}^{M} \ddot{d}_k \varphi_{2k} + g\sum_{k=1}^{M} d_k \frac{\partial \varphi_{2k}}{\partial n} + a_s(t)r = 0\,.$$

Due to validity of relation (31) on the surface S_0 the equality given above takes the form

$$\sum_{k=1}^{M} \ddot{d}_k \varphi_{2k} + \sum_{k=1}^{M} \chi_k^2 d_k \varphi_{2k} + a_s(t)r = 0\,. \tag{32}$$

Accomplishing the dot product of equality (32) by φ_{2l} $\left(l = \overline{1, M}\right)$ and having used orthogonality of own modes (Gavrilyuk, 2006) we receive the system of ordinary differential equations of the second order

$$\ddot{d}_k + \chi_k^2 d_k + a_s(t)F_k = 0; \quad F_k = (r, \varphi_{2k})/(\varphi_{2k}, \varphi_{2k}); \quad k = \overline{1, M}\,. \tag{33}$$

Suppose that before applying the horizontal impulse the tank was at the state of rest. Then we have to solve (33) under zero initial conditions. The operational method is applied here to the solution of system (33).

The following values for coefficients $d_k(t), \quad k=\overline{1,M}$ are obtained:

$$\frac{d_k(t)}{Q_0}=\begin{cases} \dfrac{1}{\chi_k^2}-\dfrac{1}{\chi_k^2}\cos(\chi_k t) & 0\le t\le T \\ \dfrac{1}{\chi_k^2}-\dfrac{1}{\chi_k^2}\cos(\chi_k t)-\dfrac{1}{\chi_k^2}+\dfrac{1}{\chi_k^2}\cos\chi_k(t-T) & t>T \end{cases}$$

Substituting these coefficients in relation (30) one can obtain the time-history of the free surface elevation.

It would be noted that dynamics of both baffled and un-baffled tanks under impulse or seismic loads is governed by equations (33).

In Fig. 14 the free surface elevation in the point B with r=1.m (see Fig. 5) depending on time is shown.

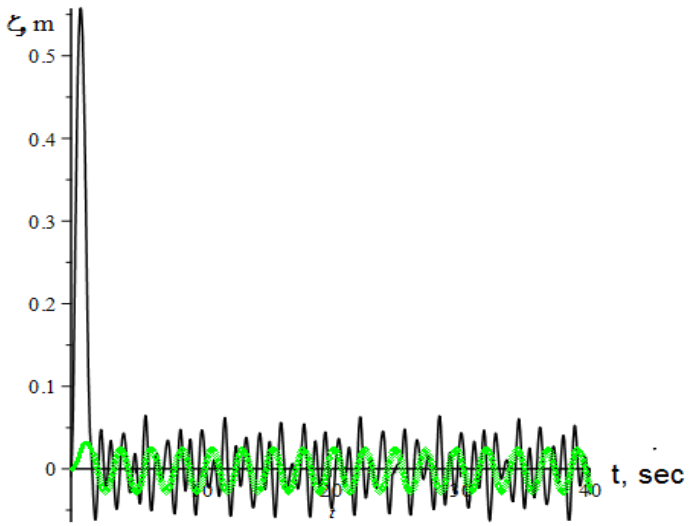

Figure 14. Time – history of the free surface elevation at the impulse load

Here the solid line denotes the free surface elevation of un-baffled tank, and dotted green line is for the tank with the ring baffle with $R_{\text{baf}}=0.3\text{m}$ installed at the height $H_1=0.8\text{m}$. It would be noted that the amplitude of the free surface elevation does not decrease by time, but has a periodic behaviour. The reason is in limitations of the proposed model for structural-vibration analysis that consists in classical dynamics of un-damped systems (equations (16), as and equation (1) are without damping matrixes). This essentially implies that all the system coordinates execute harmonic oscillation without decreasing by time.

However the results testify that installation of baffles lead to decreasing both frequencies of the liquid vibrations and the level of the free surface elevation.

11. Elasticity effects

In this section the elasticity of both bottom and walls of tanks is taken into account. Here the third system of basic functions is implied.

Modes of fluid-filled elastic shell without including the force of gravity φ_{1k} are calculated by the boundary element based method developed in (Ravnik *et al.*, 2016; Ventsel *et al.*, 2016).

It would be noted that in (Ventsel *et al.*, 2016) the vibrations of elastic hemisphere without sloshing effects were estimated.

Here we considered the cylindrical shell with a flat bottom, R = 1 m, h = 0.01 m, L = 2 m, Young's modulus $E = 2 \cdot 10^5$ MPa, Poisson's ratio $\nu = 0.3$, the material's density is ρ = 7800 kg/m^3, the fluid density ρ_l = 1000 kg/m^3, the filling level H=1.0 m. The baffle position was H_1=0.5m, and the baffle radius R_b was variable, the value R_b=0 corresponds to the un-baffled tank.

The shell is assumed to be pin-connected over its contour and boundary conditions are following: $u_r = u_z = u_\theta = 0$ to $z = 0$ and $r = R$ (clamped in the point A, Fig. 5). The own modes of the empty shell vibrations (second system of basic functions) are obtained using the finite element method as it was described in (Ventsel *et al.*, 2016).

In Table 11 the results of numerical simulation of axisymmetric frequencies (m is mode number) for cylindrical shells with elastic baffles of different radii are presented.

Table 11. Axisymmetric frequencies of elastic cylindrical shells with baffles, *Hz*

m	Empty elastic shell				Fluid-filled elastic shell			
	R_b=0	R_b=0.2	R_b=0.5	R_b=0.8	R_b=0	R_b=0.2	R_b=0.5	R_b=0.8
1	23.233	23.233	23.234	23.234	7.9259	7.5901	5.5213	1.7874
2	91.1011	91.1014	40.4818	24.4105	43.3566	42.350	15.172	9.7932
3	205.252	191.172	91.1015	91.1015	117.034	116.02	43.769	45.914
4	365.795	205.253	205.253	100.789	230.316	138.95	119.14	52.908
5	392.787	365.795	213.551	205.253	392.787	239.18	168.05	119.77

From the results obtained here one can conclude that the frequencies of fluid-filled shell vibrations are differ drastically from the frequencies of empty ones. The value R_b=0 corresponds to the un-baffled tank, and all frequencies in this case correspond to the vibrations of shell's walls. When R_b=0.2m then frequency f_1=192.172 *Hz* appears corresponded to first mode of baffle vibrations. When baffle with R_b=0.5m is installed, we observe appearance of two modes corresponded to baffle vibrations with frequencies f_1=40.4818*Hz* and f_2=213.551 *Hz* (first and second modes of baffle vibrations). At increasing the baffle radius to R_b=0.8m one can see decreasing the baffle frequencies values to f_1=24.4105Hz and f_2=100.789*Hz*. The fifth mode of the shell without baffles a torsion one, and it does not affect on fluid-structure interaction because an ideal fluid produces only a normal pressure on a moistened body.

It should be noted that installing the baffles lead to appearance of new modes with

frequencies that are lower than in the case of baffle absence.

The baffle does not affect the only first frequency of the empty tank, but it presence leads to essential decreasing the frequencies of fluid-filled shells with increasing the baffle radius.

Both elasticity effects and the size of baffles are affected essentially the values of natural frequencies.

12. Vibration analysis of elastic shells coupled with liquid sloshing

In this section we describe coupled problems of liquid sloshing and structural vibrations.

Consider the clamped-free elastic circular cylindrical shell with a flat bottom (Fig. 5) and geometrical and physical parameters described above in Section 11. The own modes of the empty shell vibrations (second set of basic functions) are obtained using FEM as it was described in (Ventsel *et al.,* 2016). Modes of fluid-filled elastic shell without including the force of gravity φ_{1k} (third system of basic functions) are calculated by method developed in (Gnitko *et al.*, 2017; Ravnik *et al.*, 2016).

To complete numerical analysis we have to obtain the first system of basic functions. For this purpose we consider the partially filled rigid cylindrical shell having the following parameters: the radius is R = 1 m, the length L = 2 m. The filling level is H=1.0 m. The baffle is considered as a circle flat plate with a central hole (a ring baffle). The vertical coordinate of the baffle position (the baffle height) is denoted as H_1. The radius of the interface surface is denoted as R_{int}, (Fig.5) and $H = H_1 + H_2$.

Fig. 15 a),b) demonstrates monotonic dependencies of the first 4 eigenvalues denoted over there as F_1,F_2,F_3,F_4, via the interface surface radius denoted by R_{int} at different baffle position H_1. Both wave numbers α=0 and α=1 are considered.

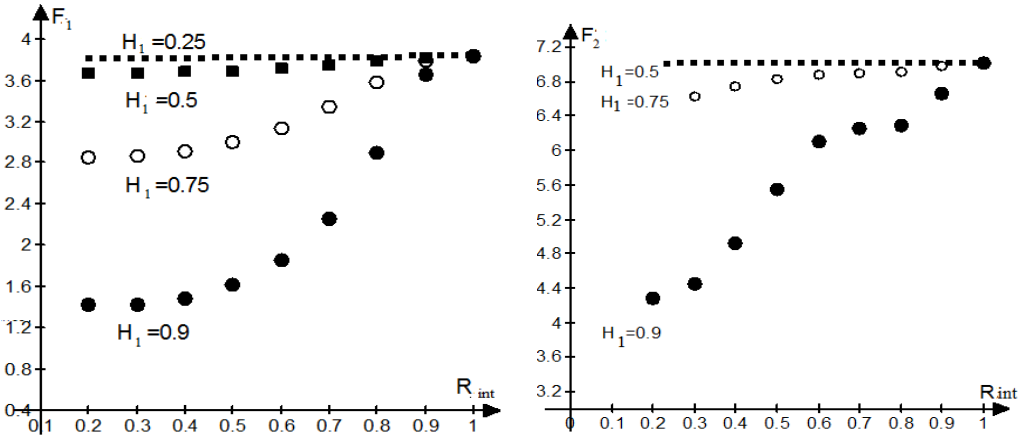

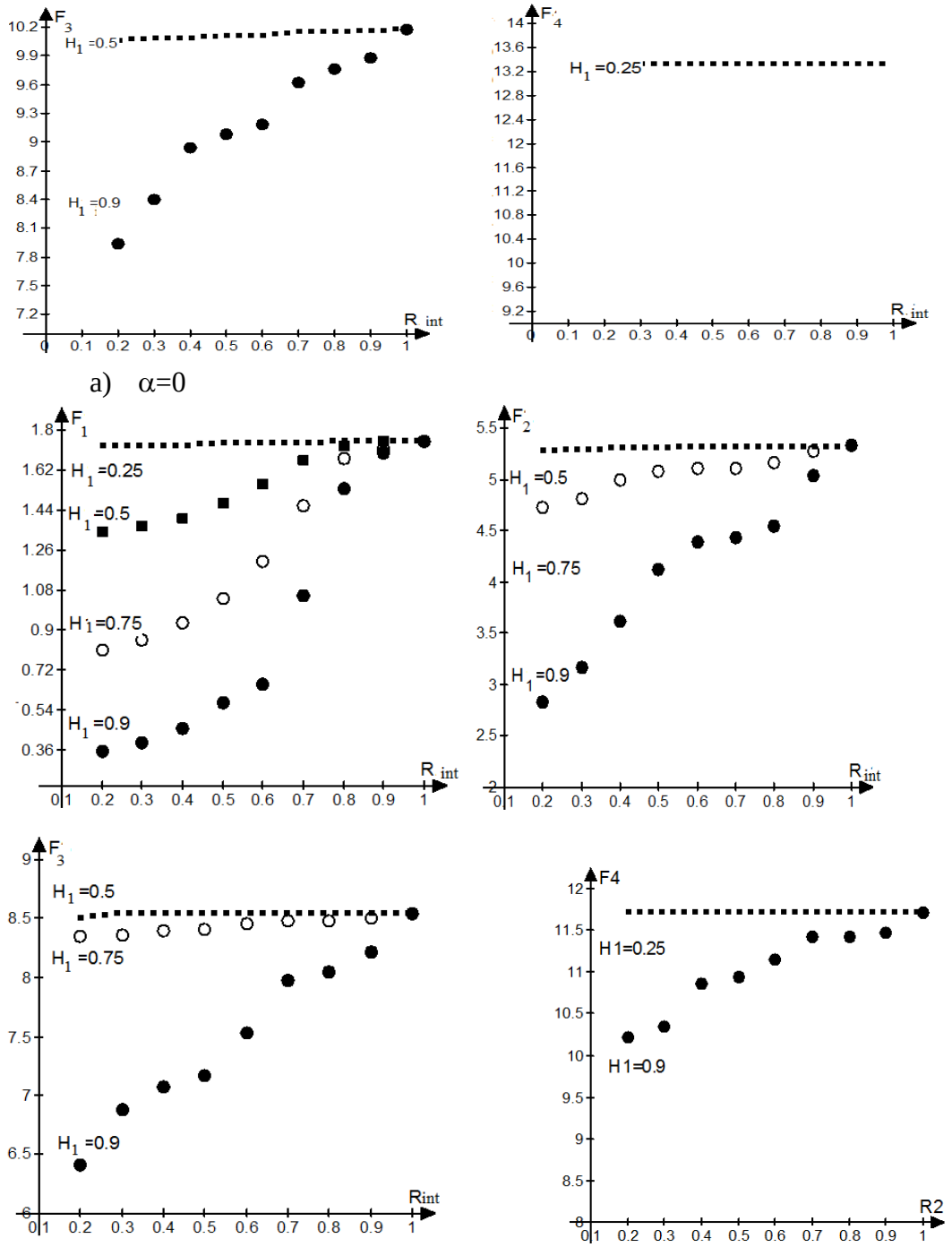

Figure 15. Eigenvalues versus R_{int} for H=1m and different H_1

From these results one can conclude that graphs of F_i as functions of R_{int} are essentially differ for different i and H_1. The presence of the baffle has affected drastically the only lower frequencies, although small baffles (when R_{int} is relatively large) do not affect the lower frequencies. This conclusion corresponds to results of Gavrilyuk et al (Gavrilyuk *et al.*, 2006).

It would be noted that the values of frequencies both for α=0 and α=1 on the left vertical border of these graphs coincide with theoretical values for tanks with solid baffles (baffles without holes) at the same values of baffle position H_1. Here we have the boundary value problem for the two-compartment tank where the lower compartment is fully-filled with the liquid. But for this compartment we have the boundary value problem with zero Newman boundary condition. It leads to the ambiguous solution, but we have known the constant potential due to the known solution for the upper compartment where the mixed boundary value problem for the cylindrical shell can be solved analytically. The liquid above the baffle behaves like a sloshing one while the liquid below behaves like a rigid one. Physically, this implies complete insulation of the upper fluid layers against inter-domain flows. On the right border of the graphs the values of frequencies coincide with ones obtained for the un-baffled tank.

When all three systems of basic function are defined, we substitute them in Equations (19) and come to solution of eigenvalue problem (20) that describes vibrations of the elastic shell coupled with liquid sloshing.

Table 12 provides the numerical values of natural frequencies of vibration for empty and fluid-filled cylindrical tanks without baffles. Here coefficients n_S, n_L indicate numbers of modes of the shell and liquid involved in coupled vibrations, n is the number of the coupled mode. For numerical simulation we have used here four shell modes and five sloshing modes.

Table 12. Frequencies of empty and fluid-filled tanks without baffles, Hz

	α =0					α =1				
n	n_S	n_L	Empty elastic tank	Fluid-filled tank	Un-coupled	n_S	n_L	Empty elastic tank	Fluid-filled tank	Un-coupled
1		1		6.1193	6.1281		1		4.0330	4.1433
2	1	1,2	23.233	7.6591	7.9259		2		7.2316	7.2316
3		2		8.2991	8.3172		3		9.1508	9.1508
4		3		9.9958	9.9958		4		10.715	10.716
5		4		11.441	11.441		5		12.071	12.071
6		5		12.723	12.723	1,2		48.520	21.902	21.955
7	2,1		91.101	43.308	43.3566	2,1		139.70	79.712	79.719
8	3,2		205.25	117.03	117.033	3,2,1		232.44	178.42	178.42
9	4,3,2		365.79	230.31	230.316	4,3		277.30	210.00	210.00

Here the sloshing frequencies are χ_n, and we calculate them using the frequency parameters χ_n^2 / g (see formula (12)). By "Uncoupled" in the Table 12 the value of frequencies are denoted that are obtained separately using first and second systems of basic functions. The interesting phenomenon here is in appearance of the first shell frequency ω_2=7.6591 *Hz* among the sloshing ones.

The main conclusions here are following. The coupling effect is more essential for axisymmetric vibrations. It also would be noted that there exist an interaction between liquid and shell vibrations. It is observed for the first shell mode. The supposition about spectrum separation of liquid sloshing and elastic structure vibrations is not valid at least when the shell bottom is considered as elastic.

The results of baffle influence are given in Table 13. The baffle with R_b=0.5m is installed at H_1=0.5m into the cylindrical shell described above.

Here numbers n, n_S, n_L are numbers of coupled mode, elastic shell mode, and sloshing mode, respectively. So one can see, which sloshing (n_L) and elastic shell (n_S) modes interfere in each coupled mode (n).

The results given here show the difference between frequencies of fluid-filled and empty shells.

Table 13. Frequencies of empty and fluid-filled tanks with baffles, Hz

n	n_S	n_L	Empty elastic tank	Fluid-filled tank	Uncoupled vibrations
1	1	1	23.234	5.5213	5.2415
2	1	1		5.9532	6.0012
3	3	2		8.2991	8.3172
4	2	3		9.9900	9.9958
5		4		11.441	11.441
6		5		12.723	12.723
7	2	1	40.4818	15.172	15.172
8	3	2	91.1015	43.769	43.769
9	4	2	205.253	119.145	119.145
10	5	2	213.551	168.052	168.052
11	6	1	365.794	196.125	196.125
12	7	2	553.183	370.881	370.881
13	8	3	572.280	401.324	401.324

But with increasing the frequency number this difference become gradually smaller. The lowest axisymmetric frequency ω_1 = 5.5213*Hz* of the fluid-filled shell corresponds to the first mode of the elastic structure. Moreover, this frequency is very close to the sloshing frequency ω_2 = 5.2415*Hz*. So the frequencies ω near 5-6*Hz* may be considered as most dangerous for the considered cylindrical shell. It will be the reason for the loss of stability.

The results testify that the supposition about spectrum separation of liquid sloshing and vibrations of the elastic structure is not valid.

Fig. 16 demonstrates different configurations of axisymmetric mode shapes of fluid-filled cylindrical shell with the ring baffle. Numeration of the modes n= 1,2, … is the same as in Table 13.

The first mode corresponds to vibrations of the shell bottom coupled with the first sloshing mode. Modes with numbers 2-6 are purely sloshing ones. The seventh mode describes baffle vibrations; eighth and tenth modes are superposition of the baffle and bottom vibrations. Ninth mode describes bottom vibrations. Modes of vibrations of vertical walls correspond to higher frequencies (n= 11-13 in Figure 16).

So coupled analysis of elastic shells vibration and liquid sloshing can reveal the complicated nature of fluid-structure interaction that is quite different for distinct tanks' shapes and fluid fillings.

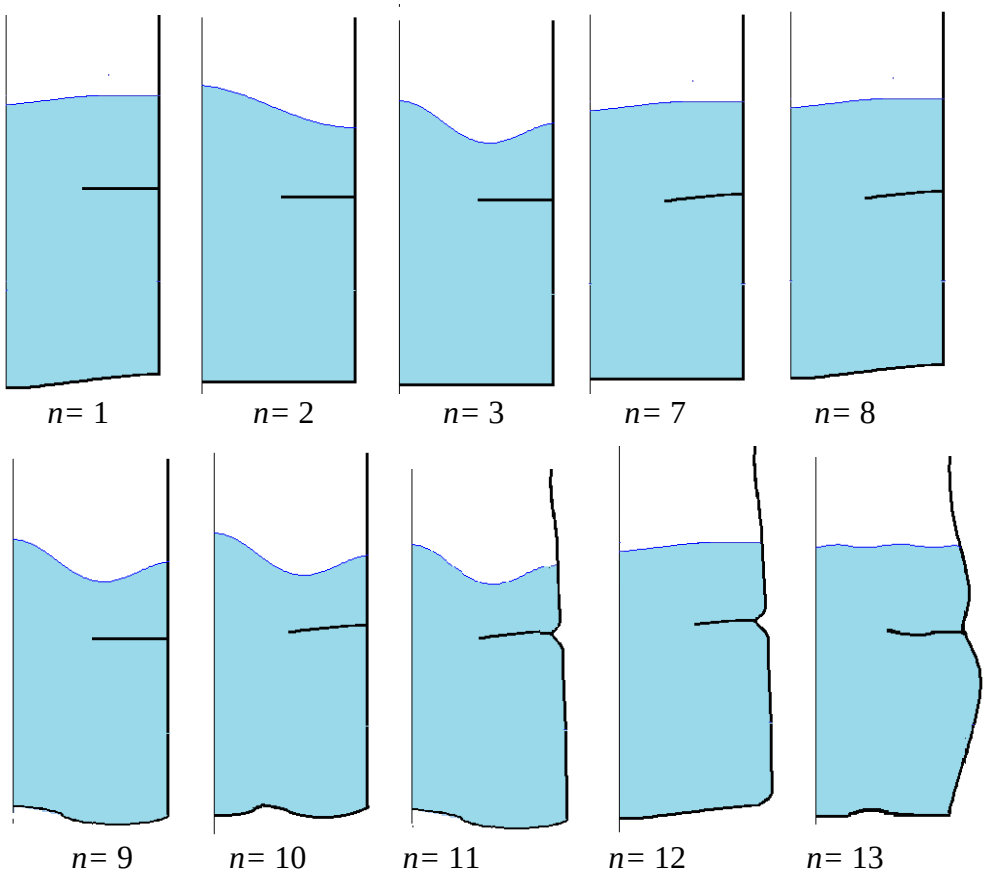

Figure 16. Mode shapes of fluid-filled cylindrical shall with the ring baffle.

13. Conclusion

The numerical method based on a coupling the finite element formulation and the boundary element method is developed for the analysis of free and forced vibrations of shells of revolution with an arbitrary meridian partially filled with the fluid. The elastic shell vibrations coupled with liquid sloshing under the force of gravity are considered.

For solving the free vibration problem for elastic shells of revolution coupled with liquid sloshing three systems of basic functions are obtained: modes of liquid in rigid

shell under force of gravity; own modes of empty shell; modes of fluid-filled elastic shell without including the force of gravity. The representation is introduced for the velocity potential as the sum of two potentials: one of them corresponds to the problem of fluid free vibrations in the rigid shell and another one corresponds to the problem of fluid-filled elastic shell vibrations without including the gravitational component. 3-D problem of determining the pressure and free surface elevation is reduced to solution of the one-dimensional system of singular integral equations. It is the basic advantage of our method based on a combination of the boundary integral equations method, finite element method and expansion into Fourier series. The forced vibration problem includes the same steps involving the liquid added masses into equations of motion. The geometry of tanks can be easy changed without complicated analytical calculations.

The proposed approach allows us to carry out the numerical simulation of frequencies and the level of the free surface elevation for baffled liquid storage tanks with baffles of different sizes and with different position in the tank considering liquid sloshing and elasticity effects. This gives the possibility of governing the baffle radius and its position within the tank at design stage.

The results of numerical simulation demonstrate that the frequencies of fluid-filled shell vibrations are differ essentially from the frequencies of empty ones, the frequencies of tanks with and without baffles are essentially different. Installing the baffle leads to a decrease of the frequencies of vibrations. The supposition about the spectrum separation of frequencies of the elastic shell filled with the liquid and sloshing frequencies in the rigid shell with the same geometrical characteristics and filling level as for the elastic one is not always valid.

The problem is solved using the one-dimensional boundary and finite element methods. This substantially reduces the computer time for the analysis and reveals new qualitative possibilities in modeling the dynamic behavior of shell structures.

The method can be extended to the non-linear sloshing problem involving different shells of revolution with two and more annular horizontal baffles.

About limitations of the method the following can be said. The proposed model for structural-vibration analysis does not involve the effects of viscosity and damping. The consideration of these effects requires new mathematical models.

14. Acknowledgment

The authors thank their collaborators on STCU Project #6247, Professors Carlos Brebbia, Wessex Institute of Technology, UK, and Alexander Cheng, University of Mississippi, USA, for their constant support and interest to our research.

References

Abramson, H.N. (2000). The Dynamic Behavior of Liquids in Moving Containers, NASA SP-106, Washington, D.C., 1966, updated by Dodge, F.T., Southwest Research Institute.

Amabili, M., Kwak, M.K. (1999). Vibration of circular plates on a free fluid surface: Effect of surface waves. *J. of Sound and Vibration*, 226(3), 407-424.

Amabili, M., Frosali, G. & Kwak, M.K. (1996). Free vibrations of annular plates coupled with fluids. *J. of Sound and Vibration*, 191(5), 825-846.

Arafa, M. (2006). Finite element analysis of sloshing in liquid-filled containers. *Production Engineering & Design for Development*, 7, 793-804.

Askari, F., Daneshmand & Amabili, M. (2011). Coupled vibrations of a partially fluid-filled cylindrical container with an internal body including the effect of free surface waves. *J. of Fluids and Structures*, 27(7), 1049-1067.

Askari, E., Daneshmand, F. (2009). Coupled vibration of a partially fluid-filled cylindrical container with a cylindrical internal body. *J. of Fluids and Structures*, 25(2), 389-405.

Bauer, H.F., Chiba, M. (2007). Viscous oscillations in a circular cylindrical tank with elastic surface cover. *J. of Sound and Vibration*, 304(1-2), 1–17.

Bermudez, A., Rodrigues, R. (1999). Finite element analysis of sloshing and hydroelastic vibrations under gravity. *Mathematical Modelling and Numerical Analysis*, 33(2), 305-327.

Biswal, K.C., Bhattacharyya, S.K. & Sinha, P.K. (2004). Dynamic characteristics of liquid filled rectangular tank with baffles. *Journal of the Institution of Engineers. India. Civil Engineering Division*, *84*(AOU), 145-148.

Brebbia, C.A., Telles, J.C.F. & Wrobel, L.C. (1984). Boundary Element Techniques, Springer-Verlag: Berlin and New York.

Crotty, J. (1982). A block equation solver for large un-symmetric matrices arising in the boundary integral equation. *Int.J. For Numerical Methods In Engineering*, 18(7), 997–1017.

Cho, J.R., Lee, H.W. (2004). Numerical study on liquid sloshing in baffled tank by nonlinear finite element method. *Computer Methods in Applied Mechanics and Engineering*, 193(23-26), 2581-2598.

Cho, J.R., Lee, H.W. & Ha, S.Y. (2005). Finite element analysis of resonant sloshing response in 2-D baffled tank. *Journal of Sound and Vibration*, 288(4-5), 829–845.

Cox David, A. (1984). The arithmetic-geometric mean of Gauss. *L'Enseignement Mathématique*, 30, 275-330.

Degtyarev, K., Glushich ,P., Gnitko, V. & Strelnikova, E. (2015). Numerical simulation of free liquid-induced vibrations in elastic shells. *Int. J. of Modern Physics and Applications*, 1(4), 159-168.

Degtyarev, K., Gnitko, V., Naumenko, V. & Strelnikova, E. (2016). Reduced boundary element method for liquid sloshing analysis of cylindrical and conical tanks with baffles. *Int. J. of Electronic Engineering and Computer Sciences*, 1(1), 14-27.

Ergin, A., Ugurlu, B. (2003). Linear vibration analysis of cantilever plates partially submerged in fluid. *J. of Fluids and Structures*, 17(7), 927–939.

Ergin, A., Ugurlu, B. (2004). Hydroelastic analysis of fluid storage tanks by using a boundary integral equation method. *J. of Sound and Vibration*, 275(3-5), 489-513.

Evans, D.V., Mclver, P. (1987). Resonant frequencies in a container with a vertical baffle. *J. of Fluid Mechanics*, 175, 295–307.

Faltinsen, O.M., Timokha, A.N. (2012). Analytically approximate natural sloshing modes for spherical tank shape. *J. Fluid Mech*, 703, 391-401.

Gavrilyuk, I., Lukovsky, I., Trotsenko, Yu. & Timokha, A. (2006). Sloshing in a vertical circular cylindrical tank with an annular baffle. Part 1. Linear fundamental solutions, *J. of Engineering Mathematics*, 54(1), 71-88.

Gavrilyuk, I., Hermann, M, Lukovsky, I., Solodun, O. & Timokha, A. (2008). Natural sloshing frequencies in truncated conical tanks. *Engineering Computations*, 25(6), 518–540.

Gedikli, A., Erguven, M.E. (1999). Seismic analysis of a liquid storage tank with a baffle. *J. of Sound and Vibration*, 223(1), 141-155.

Gedikli, A., Erguven, M.E. (2003). Evaluation of sloshing problem by variational boundary element method. *Engineering Analysis with Boundary Elements*, 27(9), 935–943.

Gnitko, V., Naumenko, V., Rozova, L. & Strelnikova, E. (2016). Multi-domain boundary element method for liquid sloshing analysis of tanks with baffles. *J. of Basic and Applied Research International*, 17(1), 75-87.

Gnitko, V., Degtyariov, K., Naumenko, V. & Strelnikova, E. (2017). BEM and FEM analysis of the fluid-structure Interaction in tanks with baffles. *Int. Journal of Computational*

Methods and Experimental Measurements, 5(3), 317-328.
Gradshteyn, I.S., Ryzhik, I.M. (2000). Table of Integrals, Series and Products, Sixth Edition, Academic Press.
Guorong, Y., Rakheja, S. (2009). Straight-line braking dynamic analysis of a partly-filled baffled and unbaffled tank truck. *I. Mech. E.*, 223(1), 11-26.
Hasheminejad, S. M., Aghabeigi, M. (2009). Liquid sloshing in half-full horizontal elliptical tanks. *J. of Sound and Vibration*, 324(1-2), 332-349.
Hasheminejad, S.M., Mohammadi, M.M. (2011). Effect of anti-slosh baffles on free liquid oscillations in partially filled horizontal circular tanks. *Ocean Engineering*, 38(1), 49–62.
Hasheminejad, S.M., Aghabeigi, M. (2011). Transient sloshing in half-full horizontal elliptical tanks under lateral excitation. *J. of Sound and Vibration*, 330(14), 3507–3525.
Hasheminejad, S.M., Aghabeigi, M. (2012). Sloshing characteristics in half-full horizontal elliptical tanks with vertical baffles. *Applied Mathematical Modelling*, 36(1), 57-71.
Housner, G.W. **(**1957). Dynamic pressures on accelerated fluid containers, *Bulletin of the Seismological Society of America*, 47(1), 15-35.
Housner, G.W. (1963). Dynamic behavior of water tanks, *Bulletin of Seismological Society of America*, 53(2), 381-387.
Ibrahim, R.A. (2005). *Liquid Sloshing Dynamics. Theory and Applications*, Cambrige University Press, 972.
Jung, M.J., Jo, J.C. & Jeong, S.J. (2006). Impact analysis of a water storage tank. *Nuclear Engineering and Technology*, 38(7), 88-102.
Kim, M.S., Lee, W.I. (2003). A new VOF-based numerical scheme for the simulation of fluid flow with free surface. Part I: New free surface-tracking algorithm and its verification. *International J. for Numerical Methods in Fluids*, 42(7), 765-790.
Kim, M.S., Park, J.S. & Lee, W.I. (2003). A new VOF-based numerical scheme for the simulation of fluid flow with free surface. Part II: application to the cavity filling and sloshing problems. *Int. J. for Numerical Methods in Fluids*, 42(7), 791-812.
Kulczycki, T., Kwaśnicki, M. & Siudeja, B. (2016). The shape of the fundamental sloshing mode in axisymmetric containers. *J. of Engineering Mathematics*, 99(1), 157-193.
Kutlu, A., Ugurlu, B., Omurtag, M.H. & Ergin, A. (2012). Dynamic response of Mindlin plates resting on arbitrarily orthotropic Pasternak foundation and partially in contact with fluid. *Ocean Engineering*, 42, 112-125.
Lamb, H. (1993). Hydrodynamics, 6th ed., Cambridge University Press.
Levitin, M., Vassiliev D. (1996). Vibrations of shells contacting fluid: Asymptotic analysis. *Acoustic Interactions with Submerged Elastic Structures*, 5, 310-332.
Lloyd, N., Vaiciurgis, E. &Langrish T.A.G. (2002). The effect of baffle design on longitudinal liquid movement in road tankers: an experimental investigation. *Trans Inst. Chem. Engrs.*, 80(4), 181-185.
Malhotra, P.K. (1997). New method for seismic isolation of liquid-storage tanks. *Journal of Earthquake Engineering and Structural Dynamics*, 26(8), 839–847.
McIver, P. (1989). Sloshing frequencies for cylindrical and spherical containers filled to an arbitrary depth. *J. Fluid Mech.*, 201, 243–257.
Miles, J.W. (1958). Ring damping of free surface oscillations on a circular tank. *J. Appl. Mech.*, 25(2), 274-276.
Naumenko, V.V., Strelnikova, H.A. (2002). Singular integral accuracy of calculations in two-dimensional problems using boundary element methods. *Engineering analysis with boundary elements*, 26(1), 95-98.
Popov, G., Sankar, S. & Sankar T.S. (1993). Dynamics of liquid sloshing in baffled and compartmented road containers. *J. Fluids Struct.*, 7(7), 803-821.
Ravnik, J., Strelnikova, E., Gnitko, V., Degtyarev, K. & Ogorodnyk U. (2016). BEM and FEM analysis of fluid-structure interaction in a double tank. *Engineering Analysis with Boundary Elements*, 67, 13-25.

Rigby, R., Aliabadi, M. (1995). OUT-OF-CORE solver for large, multizone boundary element matrices. *International Journal For Numerical Methods In Engineering*, 38(9), 1507-1533.

Ru-De, F. (1993). Finite element analysis of lateral sloshing response in axisymmetric tanks with triangular elements. *Computational Mechanics*, 12(1-2), 51-58.

Sanchez-Sanchez, H., Cortes, S.C. & Dominguez, A.M. (2004). Structural behaviour of liquid filled storage tanks of large capacity placed in seismic zones of high risk in Mexico, Proc. of 13th World Conference on Earthquake Engineering, Vancouver, B.C., Canada, 2665.

Sanchez-Sanchez, H., Cortes, S.C. (2008). Seismic response of cylindrical tanks for oil, Proc. of 14th World Conference on Earthquake Engineering, Beijing, China.

Strelnikova, E. A., Naumemko, V. V. & Gnitko V. I. (2016). Multi-domain Boundary Element Method in Nonlinear Liquid Sloshing Analysis for Fuel Tanks, Proceedings of 5th International Conference, dedicated to the 90th anniversary of Academician V. L. Rvachev, September 27-30, Kharkov : NTU "KhPI", 390-398.

Veletsos, A.S., Yang, J.Y. (1976). Dynamics of fixed-base liquid-storage tanks, Proceedings of U.S. - Japan seminar on Earthquake Engineering Research with emphasis on lifeline systems, Tokyo, Japan, November 8-12, 317-341.

Ventsel, E., Naumenko, V., Strelnikova, E. & Yeseleva E. (2010). Free vibrations of shells of revolution filled with a fluid. *Engineering analysis with boundary elements*, 34(10), 856-862.

Watson, E.B.B., Evans, D.V. (1991). Resonant frequencies of a fluid in containers with internal bodies. *J. of Engineering Mathematics*, 25(2), 115–135.